



HAL
open science

Design Strategies and Emerging Applications of High-Performance Flexible Piezoresistive Pressure Sensors

Feng Luo, Artur Ciesielski, Paolo Samorì

► To cite this version:

Feng Luo, Artur Ciesielski, Paolo Samorì. Design Strategies and Emerging Applications of High-Performance Flexible Piezoresistive Pressure Sensors. *Advanced Functional Materials*, 2026, <10.1002/adfm.75473>. <hal-05620489>

HAL Id: hal-05620489

<https://univoak.hal.science/hal-05620489v1>

Submitted on 12 May 2026

HAL is a multi-disciplinary open access archive for the deposit and dissemination of scientific research documents, whether they are published or not. The documents may come from teaching and research institutions in France or abroad, or from public or private research centers.

L'archive ouverte pluridisciplinaire HAL, est destinée au dépôt et à la diffusion de documents scientifiques de niveau recherche, publiés ou non, émanant des établissements d'enseignement et de recherche français ou étrangers, des laboratoires publics ou privés.



Distributed under a Creative Commons CC BY 4.0 - Attribution - International License

REVIEW OPEN ACCESS

Design Strategies and Emerging Applications of High-Performance Flexible Piezoresistive Pressure Sensors

 Feng Luo  | Artur Ciesielski  | Paolo Samori 

ISIS & icFRC, University of Strasbourg & CNRS, 8 allée Gaspard Monge, Strasbourg, France

Correspondence: Artur Ciesielski (ciesielski@unistra.fr) | Paolo Samori (samori@unistra.fr)

Received: 12 February 2026 | **Revised:** 26 March 2026 | **Accepted:** 2 April 2026

Keywords: flexible pressure sensors | material engineering | piezoresistive sensing mechanisms | structural design | wearable sensors

ABSTRACT

Flexible piezoresistive pressure sensors have become a keystone in emerging flexible and wearable electronic systems due to their mechanical compliance, high sensitivity, and scalable device architecture. These characteristics enabled rapid technological advances in continuous health monitoring, human–machine interfaces, soft robots, and electronic skin. Despite the considerable achievements, attaining simultaneously high sensitivity, stability, and reliability under realistic operating conditions remains challenging, requiring a unified materials- and structure-driven design paradigm. To address these challenges, this review establishes a systematic, mechanism-to-application roadmap for high-performance piezoresistive sensors. We discuss key performance metrics and fundamental sensing mechanisms, including contact resistance modulation, quantum tunneling, and percolation effects, which collectively govern the piezoresistive response. Linking these underlying physical mechanisms to macroscopic performance, we elaborate two central strategies to enhance performance: (i) materials engineering, including hybrid conductive composites, interfacial functionalization, porosity modulation, and graded multilayer designs; (ii) structural engineering like leveraging surface microstructuring, hierarchical layering, and three-dimensional conductive networks. The synergistic coupling of these strategies is illustrated through representative devices enabling health diagnostics, tactile feedback, and intelligent robotic systems. Finally, we discuss challenges and propose future research directions, including multi-modal sensing integration and on-chip intelligence, which are expected to drive the next generation of flexible electronics.

1 | Introduction

The rapid advancement of the Internet of Things (IoT) [1], artificial intelligence (AI) [2], wearable electronics [3–4], and soft robotics [5] has generated an unprecedented demand for intelligent sensing systems capable of continuous, adaptive interaction with complex environments and the human body [6–7]. Positioned at the critical interface between physics and digital electronics, pressure sensors are key components in a wide range of applications, including personalized health monitoring, immersive human–machine interfaces, and bioinspired soft robotics [8–10]. However, conventional pressure sensors

are rigid, typically composed of silicon [11] or other inorganic semiconductors [12–13], and encounter fundamental limitations when deployed on soft, deformable, or irregular surfaces such as human skin, joints, or soft robotic actuators [14]. Their intrinsic rigidity, brittleness, and planar form factors result in pronounced mechanical mismatch with soft substrates, leading to poor conformability, limited durability, and progressive signal degradation under repeated deformation. These constraints severely hinder their integration into next-generation wearable and robotic systems, where mechanical compliance, stretchability, and biocompatibility are essential for stable and reliable operation.

This is an open access article under the terms of the [Creative Commons Attribution](https://creativecommons.org/licenses/by/4.0/) License, which permits use, distribution and reproduction in any medium, provided the original work is properly cited.

© 2026 The Author(s). *Advanced Functional Materials* published by Wiley-VCH GmbH

Flexible pressure sensors have thus emerged as a transformative class of devices that combine mechanical adaptability with robust electrical functionality. According to their signal transduction mechanisms, flexible pressure sensors are generally classified as piezoresistive [15–18], capacitive [10], piezoelectric [19], or triboelectric [20]. Each sensing modality exhibits distinct advantages and inherent limitations. Capacitive sensors typically offer a highly linear response and low power consumption but are susceptible to parasitic capacitance and environmental interference, particularly humidity [21]. Piezoelectric and triboelectric sensors excel in dynamic pressure detection and self-powered operation, yet are inherently unsuitable for static or quasi-static signals [22–23]. In contrast, piezoresistive sensors transduce applied pressure into resistance variations through strain-induced modulation of conductive pathways, enabling simple device architecture, straightforward signal readout, broad pressure detection ranges, and exceptional compatibility with diverse soft materials [24–26]. Although no single sensing mechanism is universally optimal, the balance of structural simplicity, signal stability, and design versatility has established piezoresistive sensors as one of the most widely adopted platforms in flexible sensing research.

Despite substantial progress, flexible piezoresistive pressure sensors continue to face intrinsic performance trade-offs that impede their full transition from laboratory-scale prototypes to application-ready systems. Sensor key performance metrics, including sensitivity, limit of detection (LoD), sensing range, linearity, hysteresis, response/recovery times, and mechanical durability often exhibit competing dependencies rather than co-optimization [25, 27–29]. For instance, devices engineered for ultra-high sensitivity, which is crucial for detecting subtle physiological signals such as pulse waves or vocal vibrations, frequently suffer from narrow working ranges and signal saturation under moderate pressure [30]. Conversely, sensors designed for wide-range or high-pressure detection, as required in soft robotics or plantar force mapping, often compromise sensitivity, LoD, and signal resolution [31–32]. Moreover, increasing the conductive filler content to enhance electrical conductivity can stiffen the polymer matrix, reducing elasticity and ultimately leading to irreversible signal drift or mechanical fatigue during cyclic deformation [33]. The viscoelastic nature of polymeric substrates further introduces hysteresis, creep, and long-term signal instability, undermining the accuracy and repeatability required for reliable long-term operation in wearable and robotic applications [34]. Addressing these interconnected challenges requires rational materials design coupled with hierarchical structural engineering to unlock the full potential of flexible piezoresistive sensing systems.

In response, intensive research efforts have converged on two synergistic strategies for advancing flexible piezoresistive pressure sensors. The first is materials engineering [8–9, 35], which includes hybrid conductive composites, surface functionalization, porosity engineering, and multilayer conductive-gradient architectures to tailor filler dispersion, interfacial coupling, and charge-transport pathways. The second is structural design [36–38], which leverages micro- and nanostructured sensing elements, hierarchical layering configurations, and three-dimensional architectures to control stress distribution and amplify piezoresistive transduction. The integration

of these approaches has proven highly effective in mitigating traditional trade-offs, enabling devices that simultaneously achieve high sensitivity, mechanical robustness, and operational stability.

While several excellent reviews have summarized recent advances in flexible sensing from the perspectives of emerging soft materials [39–40] or specific application platforms such as electronic skins [41], a unified design paradigm bridging fundamental physics and applied systems engineering remains lacking. To fill this gap, this review establishes a systematic, mechanism-to-application roadmap for high-performance flexible piezoresistive sensors. Rather than categorizing materials and structural architectures in isolation, we emphasize their synergistic co-optimization, and illustrate how targeted engineering strategies are governed by underlying physical mechanisms to overcome intrinsic performance trade-offs (e.g., decoupling ultra-high sensitivity from linear dynamic range). By presenting this logical framework, this review aims to provide a comprehensive understanding of the design principles, performance metrics, sensing mechanisms, and optimization strategies underlying state-of-the-art flexible piezoresistive pressure sensors (Figure 1). Specifically, we (i) summarize key parameters including sensitivity, LoD, response/recovery time, linearity, hysteresis, repeatability, and durability, along with standard measurement methods; (ii) elucidate fundamental piezoresistive mechanisms based on contact resistance modulation, quantum tunneling, and conductive network percolation; (iii) highlight recent advances in materials engineering and structural design for performance enhancement; and (iv) discuss representative applications in health monitoring, human–machine interfaces, and soft robotics. Finally, we identify remaining challenges and outline future opportunities toward intelligent, adaptive, and multifunctional flexible sensing systems that will shape the next generation of flexible electronics [4, 42–43].

2 | Piezoresistive Sensing Mechanism

Engineering the piezoresistive response constitutes a pivotal strategy for realizing high-performance flexible pressure sensors, particularly those incorporating low-dimensional nanomaterials or nanostructured conductive composites [44]. This methodology transcends mere measurement of resistance variation under pressure, entailing the deliberate tailoring of materials, microstructures, and composite network topologies to precisely control the evolution of electrical resistance in response to mechanical stimuli. The observed piezoresistive behavior predominantly stems from three interdependent conduction mechanisms, which synergistically govern the macroscopic electrical response: (1) modulation of contact resistance, (2) quantum tunneling, and (3) percolation in conductive networks.

2.1 | Contact Resistance Modulation

The primary contributor to piezoresistivity is the modulation of contact resistance (R_c) at interfaces between conductive fillers or between the sensing layer and electrodes [45] (Figure 2a).

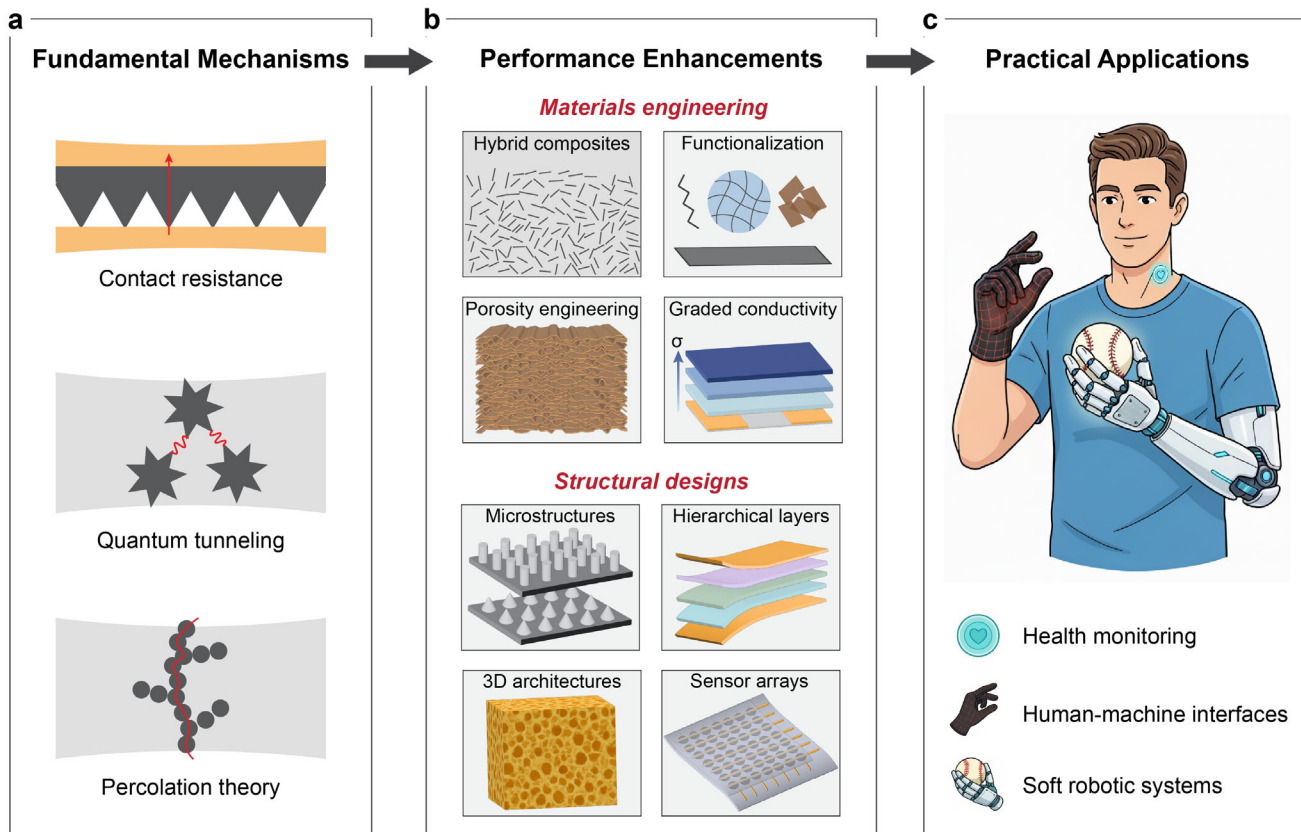


FIGURE 1 | Overview of the design pathway for piezoresistive pressure sensors, progressing from the fundamental physical mechanisms through performance enhancement strategies to demonstrations of practical applications. (a) Schematic illustration of piezoresistive sensing mechanism including contact resistance, quantum tunneling, and percolation theory. (b) Schematic overview of performance enhancement strategies, including materials engineering and structural designs. (c) Representative on-body application scenarios, including health monitoring, human-machine interfaces, and soft robotic systems.

Based on Holm's contact theory and its extensions to nanoscale regimes, R_c scales inversely with the effective contact area (A_c) and interfacial properties [46], which can be expressed as the following Equation (1):

$$R_c \propto A_c^{-\alpha} \quad (1)$$

where α is an exponent reflecting the contact type and deformation mode (e.g., elastic, plastic, or porous compression).

Upon application of external pressure, the microstructured elastomeric matrix or porous scaffold compresses, driving conductive elements into proximity. This enhances the density of conductive pathways, expands A_c by asperity flattening, and refines contact quality, thereby facilitating charge transport across these junctions [45]. Consequently, this leads to a significant decrease in the overall resistance of the conductive network. The effectiveness of this mechanism is highly dependent on the initial contact state and the geometric evolution of the interface. For instance, bioinspired microstructures, such as epidermal-like random asperities [47] or interlocked micro-dome arrays [48], serve as effective stress concentrators. Sensors fabricated from molded polydimethylsiloxane (PDMS) or polyurethane (PU) with pyramidal or hemispherical micro-features [49] demonstrate that, under subtle pressure, the sharp tips of these asperities undergo significant elastic deformation. This results in an exponential

increase in the effective contact area (A_c) and a corresponding reduction in interfacial resistance (R_c). Recent studies have further improved this strategy by introducing hierarchical nested structures that combine microscale domes with nanoscale pores, thereby enabling a broader sensitivity range through multistage contact area modulation [50–52]. This mechanism is particularly effective in highly compressible structures like aerogels or sponges, where even slight deformations can readily and significantly alter intersheet connectivity and contact topology [17].

2.2 | Quantum Tunneling Effect

Complementing ohmic contact, quantum tunneling enables charge transport across nanoscale insulating materials, especially in nanocomposites. When conductive fillers are separated by ultrathin insulating barriers or (sub)nanometer-sized voids [18], electrons can penetrate these potential barriers via tunneling, enabling current flow even without physical contact (Figure 2b). This quantum-mediated transport becomes dominant as the interfiller distance approaches the nanometer scale, where classical conduction pathways become insufficient. In this scenario, electrons can tunnel through the potential barrier between adjacent particles, and the tunneling resistance (R_t) exhibits an exponential dependence on both the insulating gap distance (d)

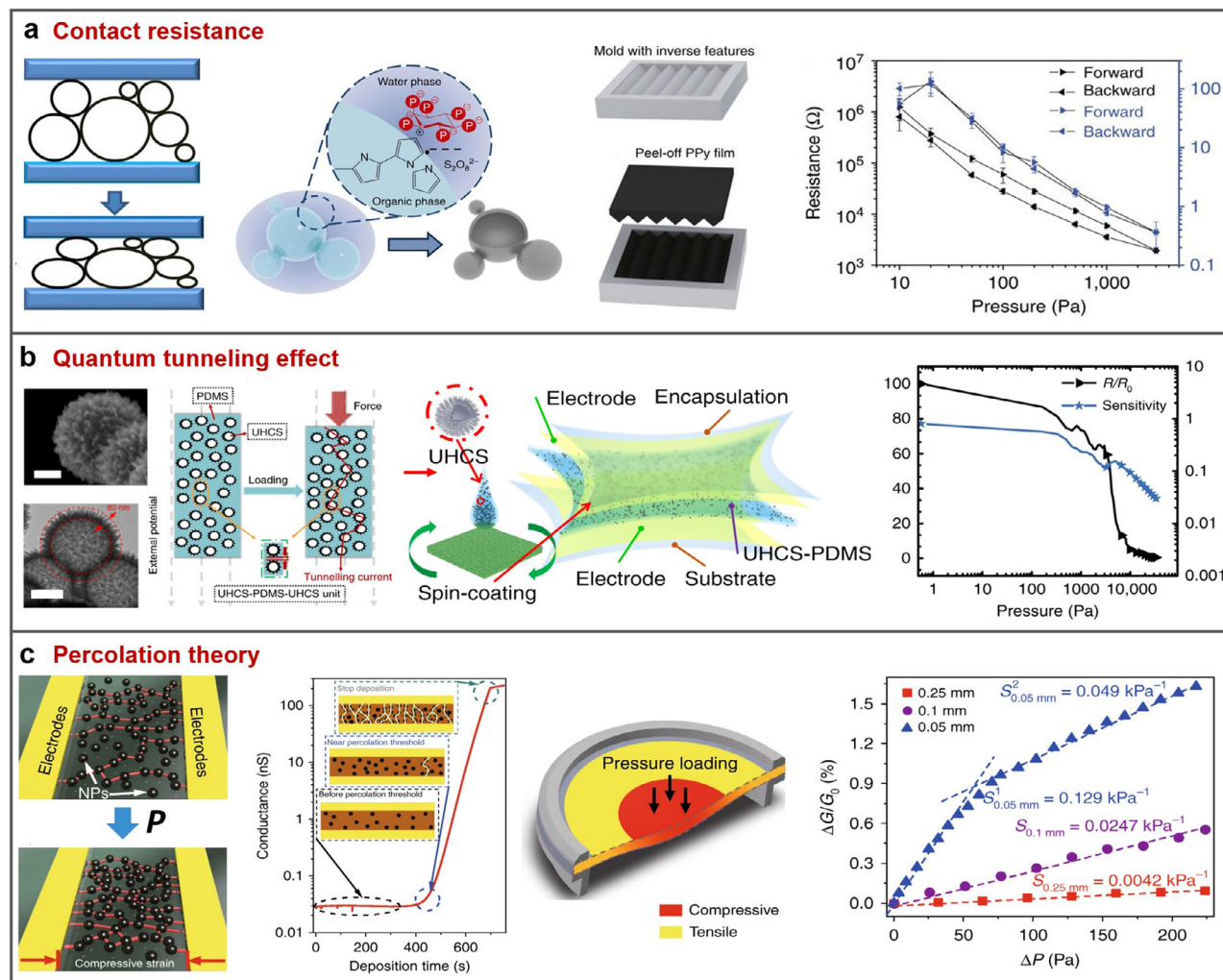


FIGURE 2 | Underlying physical mechanisms of piezoresistive responses in pressure sensors. (a) Piezoresistive behavior arising from discrete physical contacts between microstructured asperities on the sensing film and the electrode surface, modulated by applied pressure. Reproduced with permission [17] Copyright 2014, Springer Nature. (b) Piezoresistive effect governed by quantum tunneling across reduced nanogaps between urchin-like hollow carbon spheres (UHCS) embedded in a polydimethylsiloxane (PDMS) matrix. Reproduced under terms of the CC-BY license [18]. Copyright 2020, The Authors, published by Springer Nature. Scale bar: 250 nm. (c) Piezoresistive response resulting from pressure-induced reduction in interparticle spacing, which increases the number of conductive percolation pathways and alters overall electron transport. Reproduced under terms of the CC-BY license [61]. Copyright 2019, The Authors, published by Springer Nature.

and the potential barrier height (Φ_B), as described by simplified forms of the Simmons equation (2) [53]:

$$R_i \propto \exp\left(\frac{4\pi d \sqrt{2m\Phi_B}}{h}\right) \quad (2)$$

where m denotes electron mass and h is Planck's constant. Even a sub-nanometer reduction in this gap d under applied pressure can dramatically decrease R_i , resulting in a substantial increase in the overall conductivity of the material. This pronounced tunneling effect explains the exceptional sensitivity observed in nanocomposite-based pressure sensors, particularly in the low-pressure range, where tunneling dominates before physical percolation is fully established [54–55]. To deliberately exploit this effect, composites are often designed such that conductive fillers are separated by a precisely controlled nanogap. A representative example involves “urchin-like” hollow carbon spheres (UHCS)

or nanospike-textured metallic particles embedded within a thin elastomeric matrix [18, 56]. The sharp protrusions on these fillers generate localized high-electric-field regions that facilitate electron tunneling even through insulating barriers of 1–3 nm. Unlike contact resistance, which requires physical contact, tunneling current exhibits exponential sensitivity to barrier thickness, making it the dominant mechanism for detecting ultra-low pressures (e.g., <10 Pa), such as those generated by a single grain of rice or human pulse waves [57–58]. Low-dimensional nanomaterials, with their high conductivity, large surface area, and mechanical flexibility, are ideal for engineering and exploiting this quantum tunneling effect [58].

2.3 | Conductive Network Percolation

Macroscopically, electrical behavior adheres to percolation theory (Figure 2c). At conductive filler concentrations (ϕ) surpassing

the critical percolation threshold (ϕ_c), a continuous conductive network forms within the insulating matrix, enabling conduction [59–60]. Conductivity (σ) follows a power law, as shown in Equation (3):

$$\sigma \propto (\phi - \phi_c)^t \quad (3)$$

where t is a dimensionality- and connectivity-dependent component. Applied pressure prompts subtle filler rearrangements, locally elevating ϕ and reshaping network resistance.

Operating the sensor near this critical threshold is a well-established strategy for achieving ultrahigh sensitivity. As the conductive network in this regime is inherently fragile, small mechanical perturbations can either bridge or disrupt conductive paths. Such microstructural adjustments, including the formation of new conductive junctions or the reinforcement of weakly connected “bottleneck” pathways, induce large relative changes in resistance even under low pressure [61]. To optimize this percolation-controlled mechanism, several engineering strategies are commonly adopted. These include precise control of the filler loading near ϕ_c , and ensuring uniform dispersion to prevent agglomeration. The dimensionality of conducting fillers plays a pivotal role in percolative response. For instance, 1D carbon nanotubes (CNTs) [62] and 2D graphene flakes [63] are often preferred over 0D carbon black, as their high aspect ratios enable the formation of continuous networks at significantly lower percolation threshold. In such systems, applied pressure induces sliding of overlapping fillers or the “disconnection-reconnection” of conductive junctions. This behavior is particularly evident in porous 3D scaffolds (e.g., graphene foams or CNT-coated sponges) [64–65], where macroscopic compression leads to a substantial increase in the number of conductive pathways, resulting in a sensitive power-law response in resistance. Furthermore, architectural engineering, such as incorporating aligned conductive frameworks or hierarchical porous structures, helps to stabilize the percolative pathways and maintain consistent sensitivity across a broad pressure range.

Building upon this fundamental understanding about how strain modulates the contact resistance, quantum tunneling resistance, and conductive network topology, the rational design of piezoresistive sensors requires a sophisticated interplay across multiple engineering domains. This includes careful materials science, composite engineering, and structural engineering (designing specific micro/macro-architectures, such as dense films, porous foams, hierarchical assemblies, or patterned surfaces) [66–67]. The ultimate goal of this integrated engineering approach is to strategically utilize and balance the distinct yet interrelated contributions from contact resistance modulation, quantum tunneling, and percolation effects. Importantly, these mechanisms often coexist, and their relative dominance may evolve dynamically with applied pressure or strain levels. By attaining a precise control of these underlying mechanisms through sophisticated design, researchers aim to achieve the desired combination of macroscopic performance metrics, including high sensitivity, broad sensing range, rapid response time, and excellent linearity, specifically optimized for the target application requirements [68–69].

3 | Key Performance Metrics

The design, benchmarking, and optimization of flexible pressure sensors hinge on maximizing a suite of performance metrics. These include static/dynamic characteristics alongside reliability indicators, such as sensitivity, LoD, response and recovery time, linearity, hysteresis, signal repeatability, mechanical durability, and long-term stability. Each parameter provides essential insight into the operational behavior of the sensor and determines its suitability for specific wearable applications. To provide a practical and pedagogical reference for the readers, Figures 3–5 portray both idealized schematics (left panels) to define the concepts and representative experimental case studies (right panels) to illustrate the diversity of real-world testing protocols.

3.1 | Static Sensing Performance

3.1.1 | Sensitivity

Sensitivity (S) quantifies the sensor’s transduction efficiency from pressure stimulus to electrical signal (Figure 3a). For piezoresistive devices, it is generally defined as Equation (4),

$$S = \frac{(I - I_0) / I_0}{\Delta P} \quad (4)$$

where I denotes output current under applied pressure P , I_0 is the baseline current at P_0 (often 0 kPa), and $\Delta P = P - P_0$ is the pressure increment [70]. Elevated S is vital for detecting subtle physiological signals like arterial pulse waves (<2 kPa, with diagnostically relevant features in the sub-kPa range), respiratory motion, muscle contractions, and vocal fold vibrations [70–72]. S is typically derived as slopes in linear pressure segments; often segmented across different pressure ranges. Strategies to achieve high sensitivity include the use of high-aspect-ratio conductive fillers, nanoscale morphology control, and microstructured architectures that amplify pressure-induced modulation of percolating conductive networks [17].

3.1.2 | Limit of Detection

LoD, related to S , marks the minimal resolvable pressure above baseline noise (Figure 3b). It is ascertained by incremental loading, designating LoD where the signal exceeds 3× noise standard deviation. Low LoD signifies high S and minimal noise, enabling precise detection of weak biomechanical signals with high fidelity. This capability is not only essential for medical diagnostics (e.g., pulse, respiration monitoring), but also critical for advanced tactile sensing in soft robotics, prosthetics feedback systems, and human–machine interfaces where subtle pressure cues are indispensable for natural and accurate interaction [73–74]. As shown in the experimental example of Figure 3b, while LoD is formally defined by pressure (Pa), it is often practically demonstrated using minute objects (e.g., seeds or insects) to provide an intuitive weight-based (mg) resolution, which is particularly relevant for electronic skin applications.

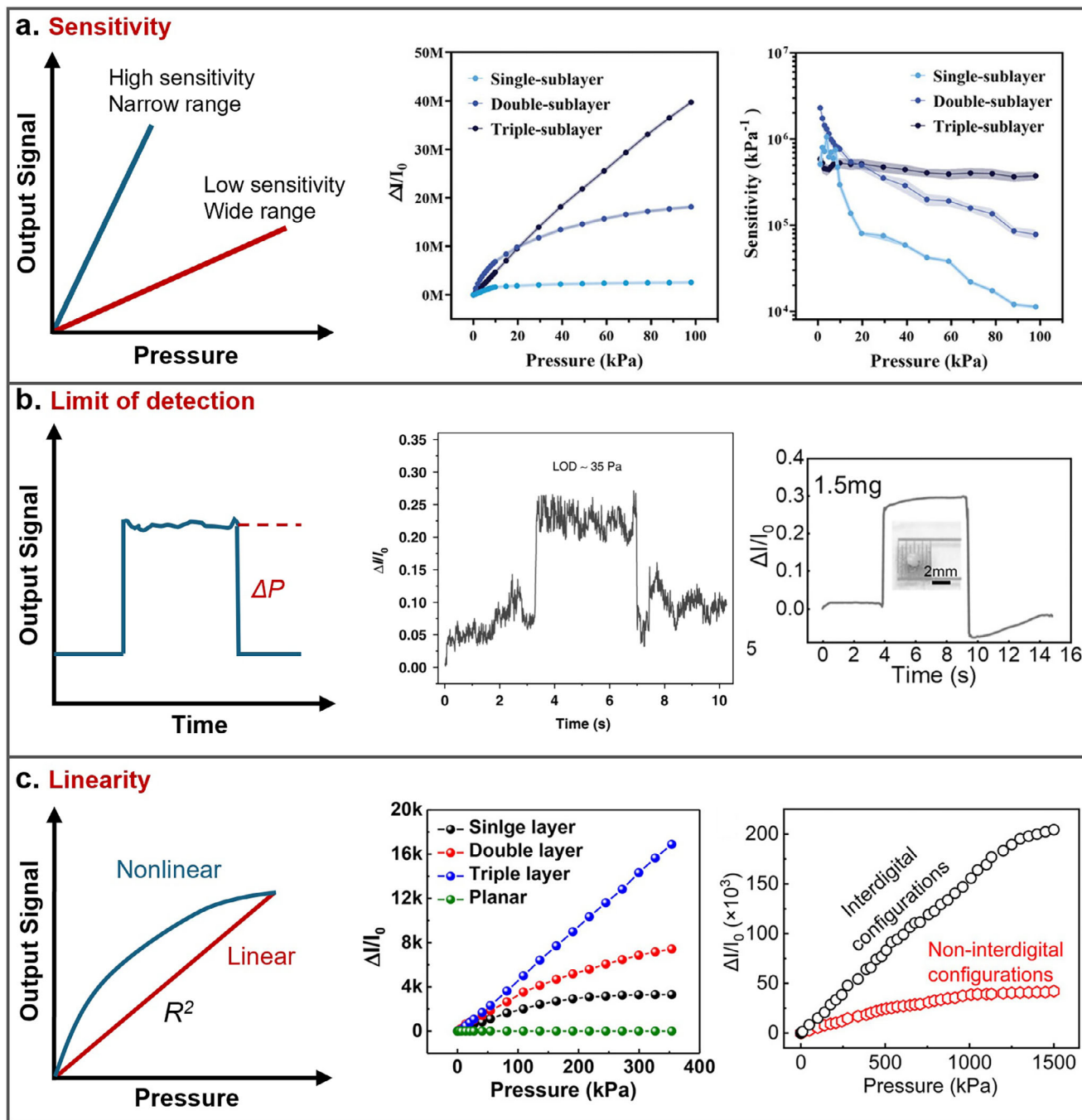


FIGURE 3 | Evaluation of performance metrics, including sensitivity, limit of detection, and response/recovery time, along with their corresponding characteristic curves. (a) Sensitivity: defined as the slope (or first-order derivative) of the output signal with respect to the applied pressure, indicating the sensor's ability to distinguish pressure variations. Reproduced with permission [76]. Copyright 2024, Wiley-VCH GmbH. (b) Limit of detection: refer to the minimum detectable pressure or corresponding weight that produces a measurable response distinguishable from the baseline noise. Reproduced under terms of the CC-BY license [62]. Copyright 2023, The Authors, published by Springer Nature. Reproduced with permission [77]. Copyright 2024, American Chemical Society. (c) Linearity: quantified by the degree to which the output signal maintains a proportional relationship with the applied pressure over the sensing range, typically evaluated via the coefficient of determination (R^2). Reproduced with permission [52, 63]. Copyright 2018 & 2023, American Chemical Society.

3.1.3 | Linearity

Linearity, defined as the extent to which a sensor's output maintains a proportional relationship with applied pressure across its operating range, is a critical performance indicator for accurate signal interpretation and quantitative reliability (Figure 3c). It

is commonly evaluated using the coefficient of determination (R^2) or the maximum non-linearity error, the latter representing the largest deviation between the measured response and an ideal linear fit, expressed as a percentage of the full-scale output [75]. High linearity is particularly important in wearable and multimodal sensing systems, where the applied pressure varies

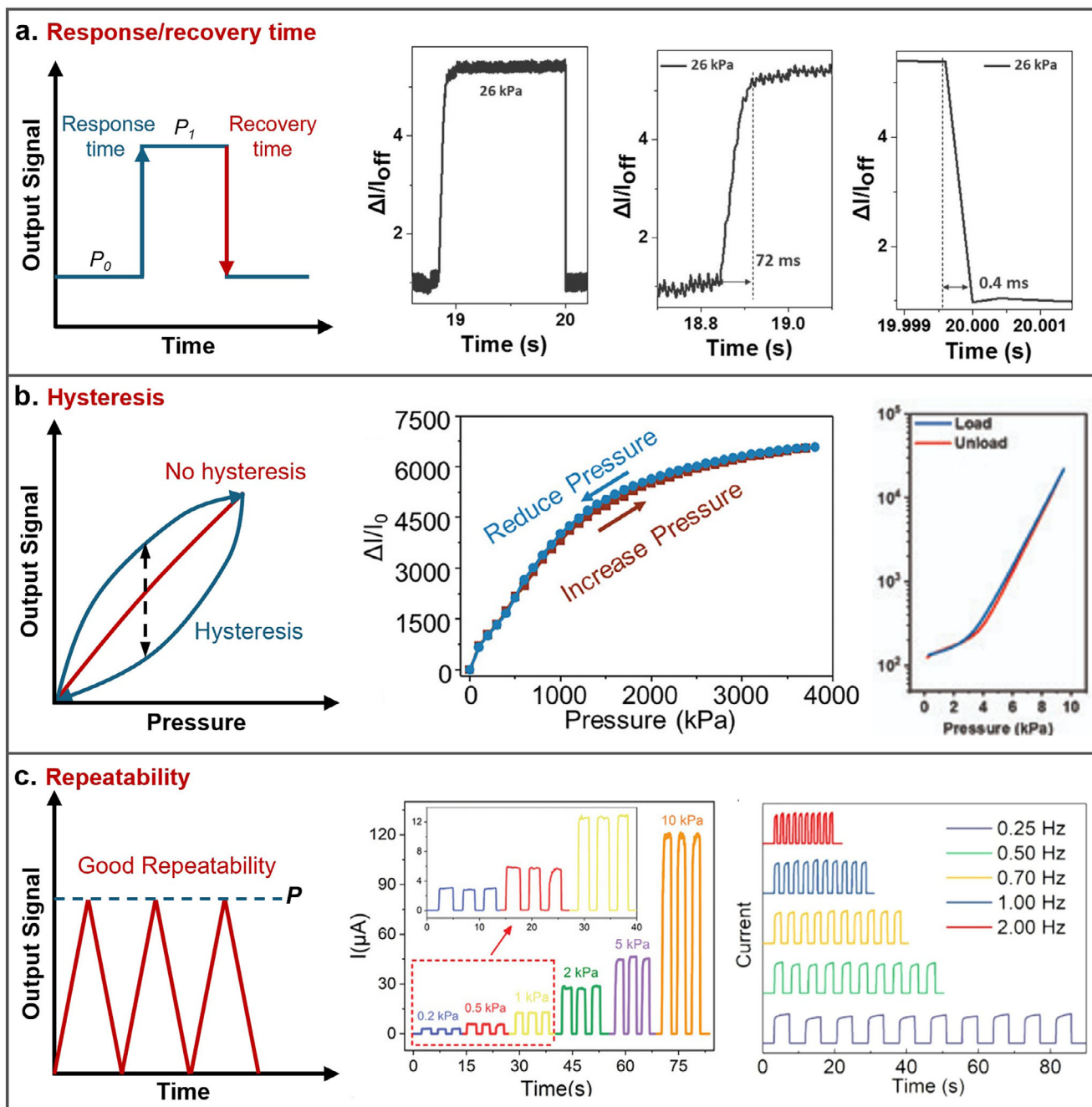


FIGURE 4 | Evaluation of performance metrics, including linearity, hysteresis, and repeatability, along with their corresponding characteristic curves. (a) Response/recovery time: defined as the time required for the signal to reach 90% of its final value during the loading and unloading processes, respectively, reflecting the sensor's dynamic performance. Reproduced under terms of the CC-BY license [88]. Copyright 2015, The Authors, published by Springer Nature. (b) Hysteresis: defined as the maximum difference in output between loading and unloading cycles at the same pressure point, reflecting signal deviation due to material lag or internal friction. Reproduced with permission [32]. Copyright 2024, Wiley-VCH GmbH. Reproduced under terms of the CC-BY license [89]. Copyright 2022, Yue Li et al. (c) Repeatability: characterized by the consistency of output signals under repeated loading/unloading cycles at the same pressure, indicating measurement reliability and stability. Reproduced with permission [90]. Copyright 2024, Wiley-VCH GmbH. Reproduced with permission [91]. Copyright 2024, Published by Elsevier B.V.

widely during human motion or physiological monitoring. A sensor with excellent linearity simplifies real-time data processing, enhances compatibility with analog and digital acquisition systems, and reduces the need for complex signal correction or recalibration procedures [36]. To improve linearity, several strategies have been proposed. A practical approach is to tune the thickness and architecture of the sensing layer to achieve multi-

stage stress distribution, effectively preventing signal saturation at high pressures while preserving proportionality under low pressures. In particular, modulating the number or stiffness of stacked sensing layers enables gradual stress dispersion through the material depth, thereby broadening the linear dynamic range [63]. Introducing hierarchical or gradient mechanical properties, such as varying cross-linking density, filler concentration, or

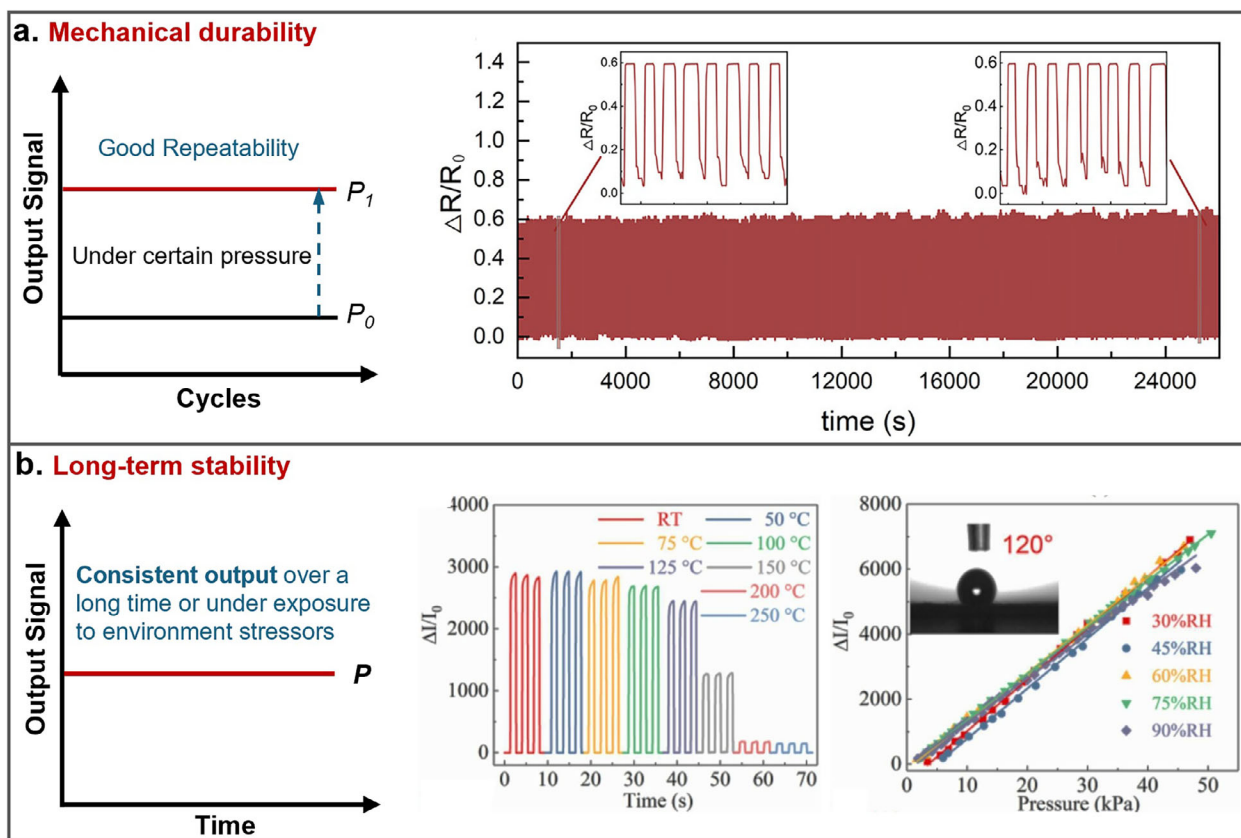


FIGURE 5 | Evaluation of performance metrics, including mechanical durability and long-term stability, along with their corresponding characteristic curves. (a) Mechanical durability: assessed by monitoring signal retention after repeated loading/unloading cycles (e.g., thousands of cycles) at a fixed pressure, indicating the sensor's resistance to mechanical fatigue and structural degradation. Reproduced with permission [93]. Copyright 2024, American Chemical Society. (b) Long-term stability: defined as the variation in output signal over an extended period under constant loading conditions and/or environmental stressors (e.g., temperature, humidity), reflecting the sensor's ability to maintain consistent performance over time. Reproduced with permission [91]. Copyright 2024, Published by Elsevier B.V.

porosity along the thickness, can further buffer abrupt load transitions and mitigate nonlinear deformation [32].

3.2 | Dynamic Response Behavior

The temporal characteristics of a flexible pressure sensor are determined by its response time (t_{res}) and recovery time (t_{rec}) (Figure 4a). Response time refers to how quickly the sensor's output signal rises following a sudden pressure input, typically quantified as the time required for the signal to reach a specified percentage (e.g., 90% or 95%) of its steady-state value. Recovery time, conversely, is the interval required for the signal to return to its baseline (or 90% of baseline) once the pressure is released [78]. In practice, these parameters are evaluated by applying stepwise loading/unloading and analyzing the transient signal curve. Together, they define the sensor's temporal resolution, which is crucial for faithfully capturing dynamic or transient biomechanical signals. Fast response and recovery are particularly important in wearable systems, where they enable real-time gait analysis, gesture recognition in HMI, or detection of physiological tremors in neurodegenerative disorders [79]. If the response or recovery is too slow, it results in signal lag, distortion of high-frequency waveform (e.g., missing pulse peaks), and misinterpretation physiological or motion data [80].

A predominant limiting factor governing the response and recovery speed of flexible pressure sensors, particularly for those employing elastomeric matrices, such as polydimethylsiloxane (PDMS), polyurethane (PU), or Ecoflex, is the intrinsic viscoelasticity of these polymers [47]. Upon mechanical deformation, polymer chains undergo segmental motion, chain uncoiling, and time-dependent stress relaxation, yielding in delayed equilibration of both the mechanical deformation and the associated electrical signal [81]. To overcome these temporal limitations, a variety of materials and structural engineering strategies have been developed to enhance sensor responsiveness. One effective approach is to reduce the thickness of the active layer, thereby shortening the relaxation path of polymer chains and enabling faster stress transmission and electrical stabilization [82]. An alternative strategy involves the incorporation of porous or microstructured architectures, such as sponge-like scaffolds, pyramidal microdomes, or air-gap configurations, which amplify stress dissipation and promote rapid recovery through expanded surface areas and optimized air flow channels [83]. Furthermore, modulating the cross-linking density and molecular weight of the elastomeric matrix affords control over viscoelastic behavior, yielding shorter relaxation times and enhanced mechanical resilience. Opting for matrix materials inherently characterized by reduced viscoelastic dissipation and elevated elasticity further contributes to improved temporal characteristics [84]. In

addition, the incorporation of lubricated or low-friction interfaces among structural components within the sensor, such as multilayered films or interlocked microfeatures, can further reduce internal energy dissipation during cyclic loading and unloading, enabling the sensor to return to its baseline state more rapidly after pressure release [75].

3.3 | Signal Reliability

3.3.1 | Hysteresis

Hysteresis is an indicator of the disparity between the sensor's output signal during the loading and unloading phases at identical pressure levels (Figure 4b). It is typically quantified as the maximum deviation between the loading and unloading curves at a given pressure point, normalized to the full-scale output [75]. This metric reflects the energy dissipation within the sensor during cyclic mechanical deformation and constitutes a principal constraint on the reliability of pressure measurements, particularly in dynamic sensing contexts. In flexible pressure sensors, hysteresis primarily originates from the viscoelastic nature of polymeric matrices, wherein time-dependent chain relaxation, segmental dynamics, and delayed elastic recovery manifest during deformation cycles [85–86]. Supplementary contributions include interfacial friction between conductive fillers and elastomer substrates, structural rearrangements within porous or percolative conductive networks, and irreversible morphological changes such as micro-pore collapse or localized plastic deformation under elevated or repetitive strain [48].

To mitigate hysteresis, researchers have developed an array of materials and interfacial engineering strategies. Employing highly elastic polymer matrices (e.g., silicone rubbers, thermoplastic elastomers) with finely tuned cross-linking densities serves to diminish internal friction and facilitate rapid elastic recovery [32, 87]. The implementation of reversible porous architectures, such as sponge-like or lattice microstructures, enhances mechanical robustness and prevents structural fatigue [30]. Moreover, interfacial optimization through low-friction coatings, lubricated interlayers, or nanoscale surface smoothing films can reduce energy dissipation at contact interfaces [75], thereby effectively suppressing hysteretic behavior.

3.3.2 | Signal Repeatability

Signal repeatability quantifies the extent to which a sensor yields consistent output responses across successive loading–unloading cycles at various pressure levels (Figure 4c). It emphasizes short-term cyclic reproducibility, typically assessed over a limited number of consecutive cycles. High repeatability signifies that the sensor's mechanical deformation and electrical transduction processes are highly reversible, exhibiting negligible drift or variability between cycles. In flexible pressure sensors, repeatability is closely related to, yet differentiable from, hysteresis behavior. Whereas hysteresis reflects the instantaneous energy dissipation during a single loading–unloading loop, repeatability reflects the cumulative consistency across multiple cycles.

Sensors exhibiting low hysteresis generally achieve superior repeatability, as minimal residual deformation or charge trapping promotes nearly identical signal trajectories under identical pressures.

To attain high repeatability, it is essential to preserve stable microstructural arrangements and reversible conductive pathways throughout cyclic deformation. In practice, this can be achieved by employing mechanically robust sensing frameworks that withstand fatigue or plastic deformation, coupled with refined adhesion between conductive layers and flexible substrates to prevent interfacial delamination or slippage. In addition, the incorporation of architectures ensuring uniform stress distribution and graded mechanical moduli can effectively suppress localized strain concentrations, thereby fostering reproducible electrical responses across different pressure magnitudes. Consequently, excellent signal repeatability is crucial for reliable biomechanical sensing, where small variations in pressure must be faithfully captured and distinguished across repetitive human motion cycles.

3.4 | Durability and Stability

Beyond instantaneous sensing characteristics, the mechanical durability and long-term operational stability of flexible pressure sensors constitute pivotal determinants of their practical reliability and lifespan in wearable applications. These attributes govern the sensor's capacity to sustain performance under persistent mechanical stress and environmental perturbations typically encountered in real-world conditions [92].

3.4.1 | Mechanical Durability

Mechanical durability refers to the sensor's capability to withstand repeated and prolonged mechanical deformation, such as bending, stretching, and compression, without undergoing irreversible structural damage or substantial performance deterioration (Figure 5a). It is commonly evaluated through cyclic loading tests (e.g., exceeding 5000–10000 cycles), wherein critical metrics including signal amplitude retention, baseline drift, and sensitivity variation are monitored [93]. In a wearable context, sensors are frequently subjected to extreme and irregular mechanical stimuli on highly deformable body sites (e.g., joints, knuckles, elbows), involving tight bending radii (<5 mm), large tensile strains (>20%), and multidirectional pressure fluctuations [94]. Mechanical failures in such scenarios often arise from cracking or fatigue of conductive networks, delamination between structural layers, or fracture of brittle components [95], leading to increased noise, hysteresis, or complete signal loss. Consequently, attaining high durability necessitates the integration of mechanically robust materials and strain-tolerant structural architectures that effectively redistribute or absorb localized stress.

3.4.2 | Long-Term Stability

In contrast, long-term stability refers to the sensor's ability to maintain consistent electrical and mechanical performance

(Figure 5b) over extended operational intervals, spanning from hours to several months, particularly under environmental stressors such as temperature fluctuations and humidity changes [91]. Stability degradation may arise from polymeric creep, cumulative fatigue, or chemical aging, including oxidation or hydrolysis of conductive fillers and polymer matrices. For instance, moisture infiltration can induce polymer swelling, perturb conductive percolation networks, or corrode metallic electrodes, thereby inducing signal drift or resistance fluctuations [96].

To mitigate these effects, reliability-enhancing strategies are widely investigated, and include the use of fatigue-resistant elastomers (e.g., Ecoflex, SEBS (styrene-ethylene-butylene-styrene)) [97] to sustain large-strain deformation, chemically inert fillers (e.g., surface-passivated MXene ($\text{Ti}_3\text{C}_2\text{T}_x$), hydrophobically modified reduced graphene oxide (rGO)) [98] to prevent oxidation or moisture attack, and stretch-tolerant conductors (e.g., Ag nanowires, CNT networks) [99] to uphold electrical continuity during mechanical stress. Structural design plays an equally critical role, wherein serpentine interconnects, graded modulus interfaces, and porous or crack-dissipating frameworks are employed to buffer local strain concentrations [100]. Furthermore, encapsulation and surface passivation layers, such as poly(chloro-*p*-xylylene) (Parylene-C), PDMS, or thermoplastic polyurethane (TPU) coatings, serve as effective barriers against humidity, oxygen ingress, and mechanical abrasion while maintaining flexibility [101]. Emerging strategies such as self-healing polymers and conductive composites are also being actively explored to further extend device longevity and functional stability [102].

Collectively, achieving superior mechanical durability and long-term stability is indispensable for guaranteeing the robust, reproducible, and sustained performance of flexible pressure sensors in real-world wearable ecosystems, thereby facilitating reliable operation for continuous health monitoring, motion tracking, and human-machine interfacing applications [103].

4 | Performance Enhancement Strategies

The pursuit of high-performance flexible pressure sensors has catalyzed extensive research across two synergistic domains: (1) materials engineering, which emphasizes nanoscale property modulation and interfacial optimization; and (2) structural design, which prioritizes optimization at the micro- and macro-scales. These strategies are inherently intertwined, aiming to overcome the inherent trade-offs between the performance metrics of sensitivity, sensing range, linearity, and durability.

4.1 | Materials Engineering

Materials engineering lays the foundation for performance enhancement by enabling precise control over the electrical, mechanical, and electromechanical characteristics of the sensing layer. This strategy involves the development of advanced functional nanomaterials, their strategic surface modification, and the hierarchical assembly forming hybrid composites.

4.1.1 | Hybrid Composites

The formulation of hybrid composites, which synergistically integrates conductive nanofillers within insulating elastomeric matrices, represents the most fundamental and widely adopted strategy for fabricating flexible piezoresistive sensors (Figure 6). The core concept of this strategy is to design a material that integrates the best of both worlds: a soft polymer matrix that imparts flexibility, stretchability, and mechanical resilience, and a dispersed conductive phase that establishes an efficient electromechanical transduction network. This hybrid design effectively decouples the mechanical and electrical functions, allowing for a degree of independent tuning that is impossible to achieve in a single, monolithic material.

The efficacy of this approach critically depends on the selection and combination of conductive fillers and polymer matrices from the vast library of available materials. Conductive components can be broadly categorized into categories such as (i) carbonaceous nanofillers like graphene derivatives (e.g., rGO flakes, graphene nanoplatelets (GNPs)) [104] and carbon nanotubes (single- or multi-walled) [57], (ii) metallic nanostructures [56, 61] such as silver nanowires (AgNWs) or gold nanoparticles (AuNPs), (iii) emerging 2D materials like MXenes (e.g., $\text{Ti}_3\text{C}_2\text{T}_x$) [105], and (iv) conductive polymers such as poly(3,4-ethylenedioxythiophene) polystyrene sulfonate (PEDOT:PSS) [106]. These fillers are typically dispersed within soft, high-elongation elastomeric matrices, including PDMS, PU, Ecoflex, or SEBS, to ensure overall device conformability.

At the microscopic level, the operating principle of these composites relies on the formation of dynamic conductive networks. Under mechanical deformation, the macroscopic resistance of the composite changes due to the combined effects of contact resistance modulation between adjacent fillers, alterations in the inter-filler distance that govern quantum tunneling, and the large-scale rearrangement or disruption of the percolation network [56, 61]. Pivotal to this design is its inherent tunability; through methodical variation of parameters including filler type, its aspect ratio, loading concentration, and spatial distribution, researchers can precisely engineer the composite's electromechanical response, including its Young's modulus, sensitivity, and linear working range, thereby tailoring it for specific applications from wearable health monitoring to robotic tactile systems [104]. However, this approach entails some challenges, as achieving a uniform dispersion and balancing the trade-off between high conductivity and mechanical flexibility remains a primary hurdle, which is a challenge that subsequent materials engineering strategies aim to address.

4.1.2 | Surface Functionalization

A fundamental challenge in fabricating high-performance piezoresistive composites is the inherent thermodynamic incompatibility between conductive nanofillers and insulating elastomeric matrices. This incompatibility typically results in weak interfacial adhesion, promoting critical microscopic

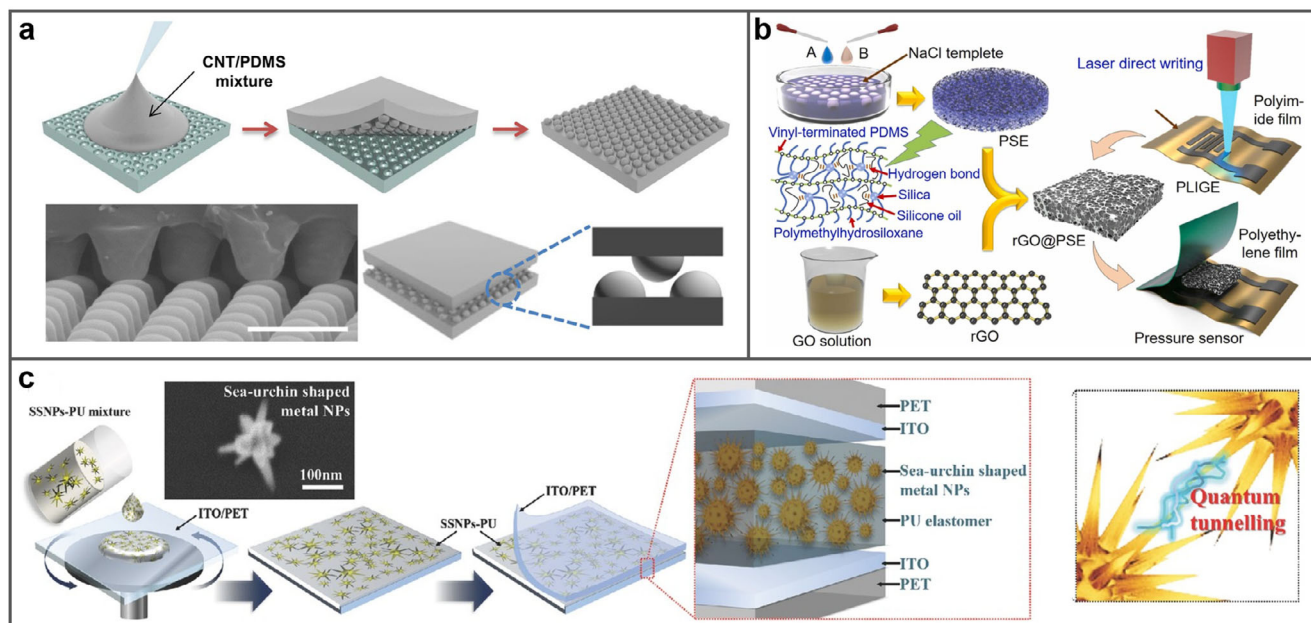


FIGURE 6 | Performance enhancement based on the materials engineering strategy of multiphase composites. (a) Conductive CNT fillers dispersed in a PDMS elastomer matrix to construct percolated composite networks. Reproduced with permission [57]. Copyright 2014, American Chemical Society. Scale bar: 5 μm . (b) GO embedded within a template-assisted porous PDMS sponge to enhance compressibility and mechanical resilience. Reproduced with permission [104]. Copyright 2024, Elsevier B.V. (c) Sea-urchin-like metal nanoparticles incorporated into PU elastomer to boost conductivity and facilitate quantum tunneling pathways. Reproduced with permission [56]. Copyright 2016, WILEY-VCH Verlag GmbH & Co.

flaws like nanofiller agglomeration and inefficient stress transfer. Ultimately, these defects severely degrade the sensor's performance, leading to low sensitivity, significant signal hysteresis, and poor long-term repeatability.

To overcome this critical bottleneck, surface functionalization has emerged as a powerful strategy for engineering the filler-matrix interface with molecular precision, as shown in Figure 7. This strategy is broadly applicable to a wide range of conductive nanofillers, from carbon-based materials like carbon nanotubes [107] and graphene oxide [58, 108] to metallic nanowires [109] and 2D MXenes [110–111]. The approach can be broadly categorized into covalent and non-covalent pathways. Covalent functionalization yields strong, irreversible covalent bonds that create a robust “molecular bridge” between the filler and matrix [58], ensuring superior adhesion and stress transfer. Noncovalent approaches, conversely, utilize weaker reversible interactions like π - π stacking or electrostatic polymer wrapping to improve dispersion while crucially preserving the intrinsic and often superior electrical properties of the nanofillers [112]. Graphene derivatives, with their abundance of surface functional groups, serve as a particularly versatile platform for both types of modification [58, 108, 112].

The profound impact of a well-engineered interface can be directly linked to the enhancement of the fundamental piezoresistive mechanisms. Primarily, by preventing agglomeration and promoting uniform dispersion, functionalization is indispensable for obtaining a stable and robust percolation network, which provides reliable conductive pathways critical for a consistent baseline and high signal repeatability [63, 112]. Secondly, the strengthened interfacial adhesion functions as a microscopic “restorative force,” preventing irreversible sliding and debonding

between fillers and the matrix during deformation cycles [113]; this enhanced microscopic reversibility is a primary reason for the significant reduction in hysteresis. Finally, by facilitating charge carrier transport across these newly engineered boundaries and reducing electronic trap states [58, 114], functionalization strengthens the overall electromechanical coupling of the composite. In essence, this strategy transforms the filler-matrix interface from a passive, problematic boundary into an active, integral component of the sensing system, providing a bottom-up approach to simultaneously enhance sensitivity, minimize hysteresis, and ensure the long-term stability of the device.

4.1.3 | Porosity Engineering

Porosity engineering is a powerful strategy that focuses on the creation and precise control of micro- and nanoscale porous structures within sensing materials (Figure 8a–c). The primary objective of this approach is to transform the material's mechanical flexibility while enhancing its electrical response to external stimuli. A variety of fabrication methods, including freeze-drying (lyophilization) of precursor hydrogels [115], sacrificial templating using removable agents (e.g., Ni foam, sugar, polymer microbeads) [116], gas foaming [117], electrospinning [118], and phase separation techniques [76], are widely employed to construct these porous scaffolds with adjustable morphology. The resulting architectures, such as aerogels, sponges, and nanofibrous networks, exhibit a markedly lower effective Young's modulus and enhanced compressibility compared to their dense, bulk counterparts.

This engineered flexibility or softness directly accounts for the enhanced sensing performance of porous materials. Under the

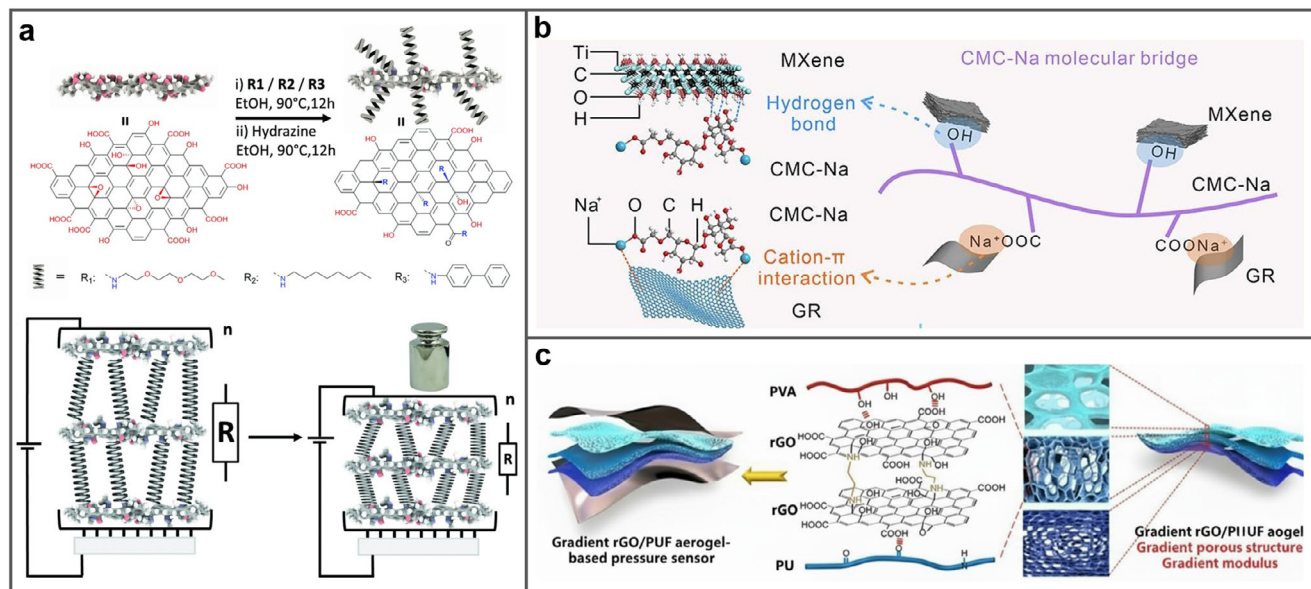


FIGURE 7 | Performance enhancement based on the materials engineering strategy of surface functionalization. (a) Covalent functionalization of GO with molecular chains of varying flexibility to modulate interlayer spacing and bulk compressibility. Reproduced with permission [58]. Copyright 2018, Wiley-VCH Verlag GmbH & Co. (b) Noncovalent functionalization of GO and MXene via sodium carboxymethyl cellulose (CMC-Na) molecular bridges to improve dispersion stability and interfacial coupling. Reproduced with permission [112]. Copyright 2024, Elsevier B.V. (c) Hybrid hydrogel constructed by covalent crosslinking of GO with ethylenediamine (EDA) and noncovalent crosslinking with polyvinyl alcohol (PVA) and PU, yielding elasticity and robustness. Reproduced with permission [108]. Copyright 2022, Wiley-VCH GmbH.

applied pressure, the substantial and reversible deformation of pores (e.g., collapse, wall bending, or buckling) results in a significant modulation of the internal conductive network. These structural shifts greatly expand the contact area, compact the conductive pathways, and reduce the quantum tunneling gaps between conductive components [119–120]. Such an enhancement process yields highly sensitive piezoresistive behaviors, particularly in the low-pressure regime. Furthermore, structural features including pore dimensions, complexity, and interconnectivity significantly affect the sensor's operational dynamics, durability against fatigue, and wearer comfort, particularly in wearable and epidermal applications, where breathability and conformability are essential [30, 121]. Overall, porosity engineering offers an effective route to separate sensitivity from inherent rigidity, enabling reliable, low-hysteresis detection over broad pressure ranges.

4.1.4 | Multilayered Conductive Gradients

A fundamental limitation in conventional sensors based on single-layered nanomaterials is the inherent incompatibility between high sensitivity and maintaining a broad linear dynamic range. Materials exhibiting high sensitivity frequently saturate at modest applied pressure, thereby limiting their effective operational regime. Multilayered architectures featuring conductive gradients emerge as an advanced design paradigm to mitigate this challenge, wherein stacked layers with progressively modulated conductivity or mechanical properties are integrated into a unified sensing architecture (Figure 8d,e) [63, 122]. A representative configuration typically incorporates a base layer exhibiting low conductivity, serving to suppress baseline current and mechanical noise, and a highly conductive top layer that amplifies

signal output under pressure-induced deformation [28, 32]. Each layer engages sequentially under increasing pressure, allowing progressive activation that extends the sensing range while maintaining excellent linearity across wide pressure regimes [28, 32, 114].

Such multilayer systems can be fabricated through sequential deposition (e.g., layer-by-layer coating or casting), controlled gradient interdiffusion, or in situ polymerization with a graded concentration of nanofillers [32, 76]. By carefully engineering the vertical gradients in conductivity and stiffness across the interfaces, researchers can precisely tailor the sensor's response profile. This design not only enhances sensitivity and signal reproducibility but also provides a powerful and versatile framework for creating application-specific sensors, capable of everything from ultra-sensitive touch detection to robust, large-range biomechanical monitoring.

4.2 | Structural Designs

Complementary to materials engineering, which refines the intrinsic properties of the sensing material, structural design offers an equally powerful framework for enhancing sensor performance. This approach focuses on shaping, patterning, and assembling the sensor components at the micro- and macro-scales. By creating specific geometries, engineers can precisely manipulate stress concentration and control deformation pathways within the device. This allows for a dramatic amplification of the signal transduction efficiency, tailoring of the response characteristics, and the introduction of entirely new functionalities that go beyond the inherent capabilities of the constituent material. Such strategies are essential for bridging

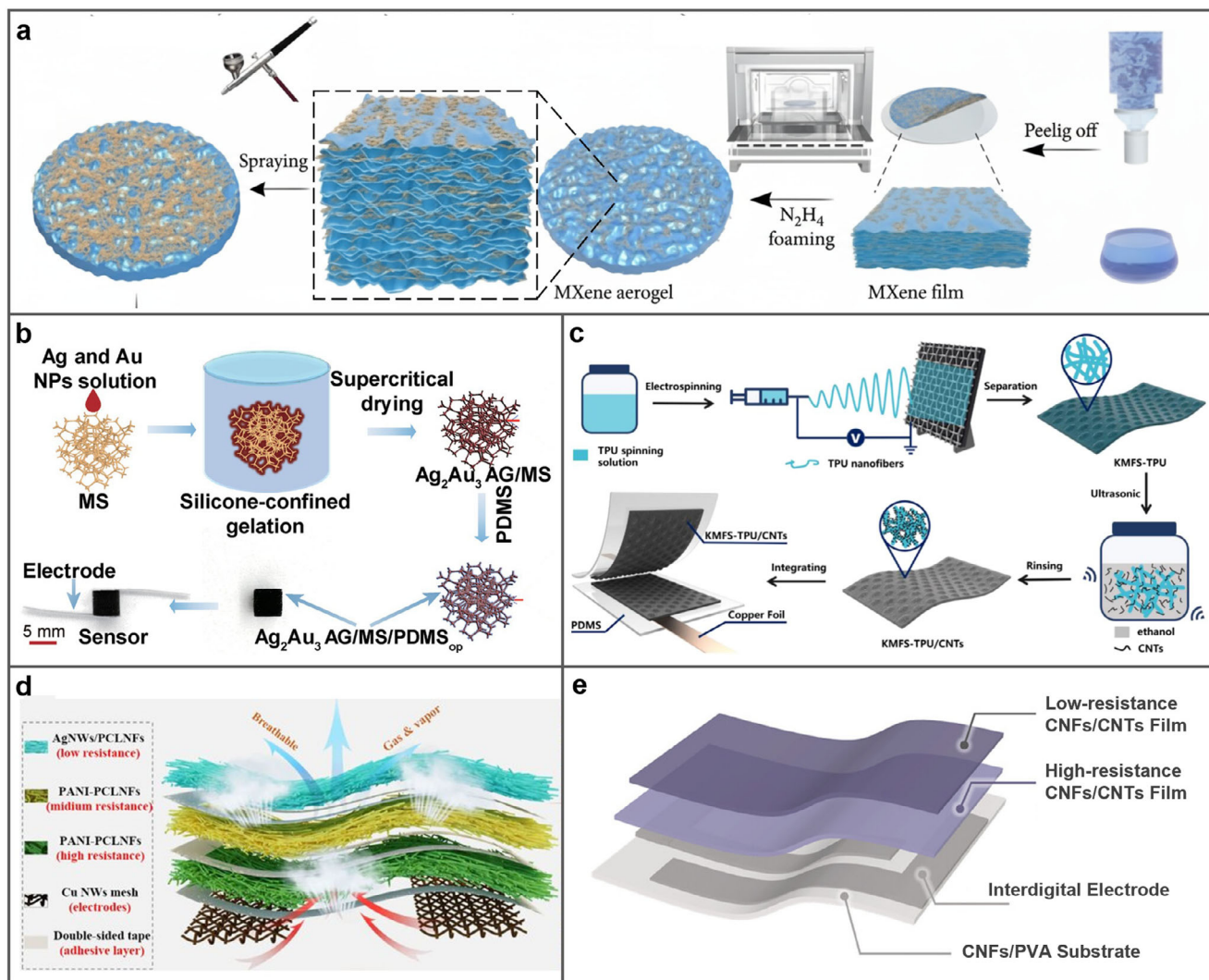


FIGURE 8 | Performance enhancement based on materials engineering strategies, including porosity engineering (a–c) and multilayer architectures (d,e). (a) Dense MXene films converted into porous structures via gas foaming with N_2H_4 vapor. Reproduced under terms of the CC-BY license [117]. Copyright 2022, Yongfa Cheng et al. (b) Conductive metal nanoparticles deposited onto melamine sponge (MS), followed by PDMS encapsulation to preserve porosity and conductivity. Reproduced under terms of the CC-BY license [123]. Copyright 2022, The Authors, published by Wiley-VCH GmbH. (c) CNTs coated on electrospun porous TPU films to create flexible conductive networks. Reproduced with permission [118]. Copyright 2021, Elsevier B.V. (d) Triple-layered nanofiber films with a conductivity gradient to improve output sensitivity. Reproduced with permission [50]. Copyright 2023, Tsinghua University Press. (e) Bilayer CNFs/CNTs films with contrasting conductivities to enhance both sensitivity and linearity. Reproduced with permission [32]. Copyright 2024, Wiley-VCH GmbH.

the gap between intrinsic material properties and overall device performance.

4.2.1 | Surface Microstructuring

Surface microstructuring is a powerful design strategy that directly overcomes the attenuated responsiveness inherent to planar sensors through the incorporation of well-defined, three-dimensional architectures (Figure 9a), including pyramids, domes, pillars, ridges, gratings, or wrinkles, onto the active sensing layer or electrodes [8, 37–38]. The fundamental principle of this approach is stress concentration, where applied external pressure, rather than dispersing uniformly across large area, is concentrated onto the external features of these microfeatures,

leading to significant and highly localized deformation modes like bending or buckling [124–125]. This process dramatically amplifies the microscopic changes within the conductive network, generating a large and clear electrical signal that is especially pronounced in the low-pressure regime. The realization of these intricate topographies is enabled by a range of microfabrication techniques, from high-precision photolithography [124] and laser ablation [88] to versatile and cost-effective soft lithography (e.g., PDMS molding) [126], template-assisted molding [127], and 3D printing [128]. Crucially, this approach offers a high degree of tunability; by systematically engineering design parameters such as the geometry, density, and aspect ratio of the features, researchers can rationally design the sensor's response curve to meet the specific demands of a target application [124–125, 128].

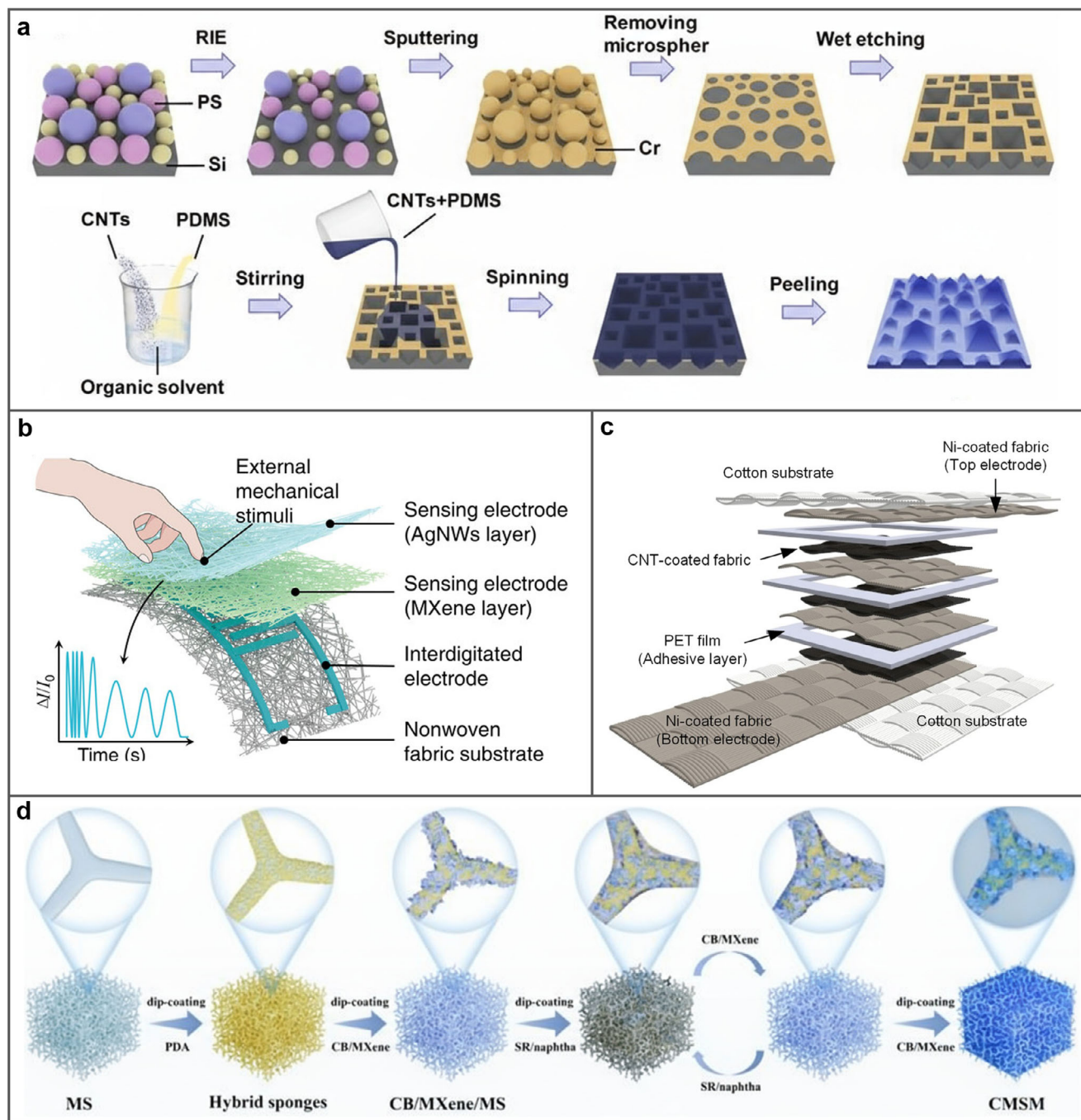


FIGURE 9 | Performance enhancement strategies based on structural design strategies, including microstructuring, multilayered, and 3D architecture. (a) Hierarchical microstructures replicated from etched silicon templates using CNT/PDMS dispersions. Reproduced with permission [49]. Copyright 2024, American Chemical Society. (b) Fibrous layered structures based on nonwoven fabrics loaded with conductive nanomaterials. Reproduced with permission [135]. Copyright 2023, Wiley-VCH GmbH. (c) Multilayered Ni-coated cotton fabrics integrating with insulating spacers to boost sensing performance. Reproduced with permission [51]. Copyright 2019, Wiley-VCH Verlag GmbH & Co. (d) 3D sponge architecture subsequently coated with carbon black (CB)/MXene composites as active sensing elements. Reproduced with permission [141]. Copyright 2025, American Chemical Society.

Furthermore, the concept of surface microstructuring extends beyond mere sensitivity enhancement, facilitating the realization of multifunctional devices. Through the engineering of interdigitated configurations, such as complementary arrays of micro-pyramids or gecko-inspired micro-textures, highly stable and reproducible mechanical interfaces can be established. Such interlocking architectures prevent lateral slippage between sens-

ing layers during repeated pressure cycles, a common cause of signal drift, thereby significantly improving the sensor's long-term reliability. Moreover, such structured interfaces can enable multi-directional force sensing [57, 125]. Orthogonal loads cause compressive deformation of the structures, whereas parallel (shear) force induces a distinct bending or twisting motion. These different deformation modes generate unique and

distinguishable electrical signatures, allowing the sensor to differentiate between pressure and shear forces.

In practical wearable scenarios, pressure sensors are inevitably exposed to coupled mechanical deformations (bending, stretching, and compression), which can introduce motion artifacts and distort the pressure readout. A first and robust route is geometry-enabled mechanical decoupling, where the pressure-sensing element is mechanically isolated from the tensile/bending neutral plane via structural buffers (e.g., stiff frames/rigid islands [129], serpentine interconnects [130], micropore/isolation layers, air-gap or spacer layers [131], and region-separated layouts [132]). Such designs suppress strain transfer into the active pressure-sensing region while preserving compressive compliance. Complementarily, algorithmic decoupling can be implemented when multi-channel outputs are available (e.g., resistance and capacitance in hybrid transduction [133], or stacked pressure/strain layers [134]). In this approach, calibration-based regression or lightweight machine-learning models map the coupled signals into decoupled pressure and deformation components, enabling reliable pressure inference under concurrent bending/stretching. These combined geometry-and-algorithm strategies are increasingly important for real-world wearable deployments and for extending multidirectional tactile sensing toward interference-robust operation.

4.2.2 | Engineering Through Hierarchical Layering

While single-layer sensors offer simplicity, they often force a compromise between conflicting material requirements. For example, a material optimized for maximum piezoresistive sensitivity may be mechanically fragile, environmentally unstable, or possess poor electrical contacts. Hierarchical layering engineering is a sophisticated structural design strategy that overcomes this challenge by adopting a multilayer stack architecture [51, 135], where each layer is specifically engineered to fulfil a distinct functional role (Figure 9b,c). This approach is analogous to a “division of labor” at the device level, allowing for the effective separation and independent optimization of sensing, mechanical, electrical, and protective functionalities [135–136] that would be impossible to achieve within a single, monolithic material.

A typical hierarchical sensor is a rationally designed integrated system. It commonly comprises a highly responsive piezoresistive sensing layer at its core, paired with an elastic or viscoelastic buffer layer that modulates dynamic deformation, provides mechanical damping to reduce signal overshoot, or acts as a stress-absorbing foundation [25]. This is then interfaced with robust and flexible electrode layers engineered for stable electrical readout [137]. The entire stack is often supported by a substrate that enhances structural integrity and facilitates integration with other systems. Finally, a durable encapsulation layer can be added to protect the sensitive core from moisture, chemical exposure, and mechanical abrasion, significantly enhancing the device's operational lifetime.

This multilayer configuration provides a powerful framework for achieving synergistic performance optimization. It allows, for instance, for the safe use of an ultra-sensitive but frag-

ile sensing material by embedding it within tough, protective outer layers [51]. Furthermore, dynamic response characteristics, such as the sensor's sensitivity to different vibration frequencies, can be precisely tuned by introducing energy-dissipating or damping interlayers [25, 136]. The ability to add dedicated shielding or dielectric layers can also dramatically improve the signal-to-noise ratio [51, 138]. By allowing each component to excel at its specific task, hierarchical layering engineering offers a robust and versatile route to creating highly reliable, durable, and sensitive devices that effectively balance the competing demands of advanced wearable and robotic applications.

4.2.3 | Three-Dimensional Architectures

A distinct and highly effective approach to creating three-dimensional sensors involves the use of prefabricated, nonconductive 3D scaffolds that serve as a structural backbone for a subsequently deposited conductive sensing layer [139–140] (Figure 9d). This “scaffold engineering” strategy is fundamentally different from the monolithic porosity engineering discussed previously, as it decouples the mechanical properties of the structure from the electrical properties of the sensing material, providing an exceptional degree of design freedom and performance tunability. The process typically begins with a highly porous, elastic, and insulating 3D scaffold, such as a commercially available melamine [141–142] or polyurethane [64, 143] sponge, or a custom-fabricated structure made via 3D printing [66] or electrospinning [144]. This scaffold defines the overall architecture, mechanical compliance, and recovery behavior of the final sensor. Subsequently, a thin, uniform layer of a conductive material, such as a solution of graphene [64], carbon nanotubes [65], MXenes [145], or conductive polymers [142, 146], is coated onto the entire interconnected surface of the scaffold's internal framework using simple, scalable methods like dip-coating.

This “scaffold-and-coating” design yields a spatially interconnected, hollow conductive network mirroring the substrate's intricate geometry. When pressure is applied, the scaffold readily compresses, causing the conductive coatings on adjacent internal struts to make and break contact at countless microscopic points [147–148]. This massive and highly reversible modulation of contact points throughout the entire 3D volume becomes the dominant sensing mechanism, leading to ultra-high sensitivity and a very low detection limit [142–143, 149]. Given that mechanical recovery is governed by the highly resilient polymer scaffold, these sensors often exhibit exceptionally fast response times and minimal hysteresis [149]. By selecting scaffolds with different pore sizes, densities, and biomimetic morphologies (e.g., honeycomb or cellular frameworks) [66, 115, 139–140], researchers can precisely engineer the sensor's compression modulus, linear range, and fatigue resistance to meet specific application demands.

To facilitate a quantitative cross-comparison of representative material/structure combinations and their resulting figures of merit, we summarize state-of-the-art flexible piezoresistive pressure sensors in Table 1, by categorizing them in view of their material composition, structural design, sensitivity, sensing range, response time, durability, LoD, and the dominant piezoresistive mechanisms.

TABLE 1 | Cross-comparison of state-of-the-art flexible piezoresistive pressure sensors: Material/structure design, key performance metrics, and dominant mechanisms.

Material composition	Structure design	Sensitivity (kPa ⁻¹)	Sensing range (kPa)	Response time (ms)	Durability (cycles)	LoD (Pa)	Piezoresistive mechanisms	Refs.
Porous polypyrrole	Pyramid-like microstructure	56	3	50	8000	0.8	Contact	[17]
UHCS-PDMS composites	—	260.3	10	60	5000	—	Quantum tunneling	[18]
Nanoparticle film	—	0.13	40	—	500	0.5	Percolation	[61]
Conductivity gradient PEDOT:PSS	Microgroove interlocked structure	39812	1500	30	10000	0.1	Contact	[76]
MWCNT/PDMS composites	Hierarchical microstructures	1.3	200	12	10000	35	Contact	[62]
rGO/PVDF composites	Interlocked multilayers	47.7	353	20	5000	1.3	Contact	[63]
Conductivity gradient CNT/PDMS layers	Microstructure gradients	153	1300	40	20000	0.5	Contact	[52]
Conductive carbon oil film	Hierarchical Layering	636	56	130	10000	300	Contact	[89]
AgNWs/MXene-coated xylon fabrics	Hierarchical layers	1417	100	30	5000	—	Contact	[90]
MWCNTs/ILs/PU fabrics	Convex microarray	7	420	60	80000	0.1	Contact	[93]
CNT/PDMS composites	Interlocked microdomes	15	25	40	—	0.2	Quantum tunneling	[57]
Sea-urchin-shaped Metal NPs/PU layer	—	2.5	18	30	200	—	Quantum tunneling	[56]
EDA/rGO/PVA hydrogels	3D PU Foam	0.2	1	34	10000	1	Contact	[108]
3D MXene aerogel	Hierarchical layering	306	87	35	20000	2.3	Contact	[117]
CNTs/PDMS composites	Pyramidal microstructures	8775	1000	12	10000	30	Contact	[49]
MXene/AgNW modified fabric	Hierarchical multilayers	770	100	70	5000	1	Contact	[135]
Ni/CNT-coated fabric layers	Multilayers structure	26	982	83	1000	200	Contact	[52]
CB/MXene mixtures	MS foam	7	20	150	60	—	Contact	[141]

—: not reported; UHCS: urchin-like hollow carbon spheres; PDMS: polydimethylsiloxane; PEDOT:PSS: poly(3,4-ethylenedioxythiophene); poly(styrenesulfonic acid); MWCNT: multiwalled nanotube; rGO: reduced graphene oxide; PVDF: polyvinylidene fluoride; AgNWs: silver nanowires; ILs: ionic liquids; PU: polyurethane; EDAs: ethylenediamine; PVA: polyvinyl alcohol; CB: carbon black; MS: melamine sponge.

5 | Practical Applications

The rapid advancement of high-performance flexible pressure sensors has unlocked their potential for integration into a broad spectrum of wearable and smart systems. Leveraging their intrinsic flexibility, mechanical adaptability to complex body curvatures, ultrahigh sensitivity to subtle physiological or mechanical stimuli, and rapid dynamic response, these sensors serve as fundamental enablers of next-generation interactive technologies. Such attributes empower diverse and transformative applications spanning personalized health monitoring, intuitive human–machine interaction (HMI), and advanced soft robotics [83, 150–151]. In these contexts, flexible pressure sensors serve as precise signal transducers and as intelligent interfaces capable of bridging the physical and digital worlds, translating minute mechanical cues into meaningful information for real-time perception, decision-making, and actuation. The following sections summarize the representative application domains and highlight how material and structural innovations have been tailored to meet specific functional requirements across different use scenarios.

5.1 | Health Monitoring

Flexible pressure sensors have demonstrated exceptional potential for continuous, noninvasive, and personalized healthcare monitoring, with a particular propensity for operating in point-of-care settings. Their excellent conformal contact with the skin and high-fidelity detection of minute pressure fluctuations enable tracking a wide spectrum of physiological signals (Figure 10a), facilitating a paradigm shift from reactive clinical diagnostics toward preventative, real-time, and individualized health management [83]. For instance, sensors positioned over superficial arteries, such as the radial or carotid (Figure 10b), enable noninvasive and detailed acquisition of arterial pulse waveforms [152–153]. Beyond heart rate monitoring, these waveforms provide rich hemodynamic indicators including pulse transit time (PTT), augmentation index (AIx), and subtle morphological features like diastolic notch characteristics, all of which provide insight into vascular elasticity, blood pressure trends, and overall cardiovascular health [154–155]. Similarly, integrating these sensors into epidermal patches, smart textiles, or chest-mounted devices allows for continuous respiratory monitoring (Figure 10c) by detecting thoracic or abdominal expansion/contraction, or airflow near the nostrils or mouth [156–158]. The high sensitivity and fast response of these sensors enable real-time assessment of respiratory rate, breathing rhythm, and even the detection of apneic episodes or abnormal breathing patterns, whose parameters are critical importance for early diagnosis and long-term management of pulmonary diseases [157, 159]. Reliable detection of these low-magnitude signals (~1–2 kPa range) relies on tailored material engineering and microstructured sensor architectures that minimize the LoD while maintaining rapid, repeatable responses. Furthermore, the inherent flexibility and stretchability of these sensors allow seamless placement near joints (e.g., fingers, elbows, knees, spine) to track joint angles, range of motion, and subtle tremors [160]. Such measurements are invaluable for rehabilitation monitoring, objective sports performance evaluation, and early detection of movement disorders such as Parkinson's disease or osteoarthritis [161–162]. Other notable applications

include swallowing monitoring for dysphagia assessment, ocular movement tracking for neurological or HMI input [163], plantar pressure mapping in smart insoles for gait analysis (Figure 10d), diabetic foot ulcer prevention, and prosthetic limb optimizing [27, 153]. Collectively, these capabilities position flexible pressure sensors as key enablers of future wearable medical systems, offering personalized, unobtrusive, and continuous healthcare with high precision and reliability.

5.2 | Human–Machine Interfaces

Flexible pressure sensors are redefining human–machine interactions by replacing conventional rigid input devices (e.g., buttons, joysticks) with soft, continuous, and intuitive interfaces [38]. Unlike robotic e-skins that primarily endow machines with artificial tactile perception, HMI-oriented sensors serve as intent-detection interfaces, enabling humans to convey commands and gestures through subtle mechanical cues (Figure 11a). These mechanical signals are then digitized into actionable control commands for physical or virtual systems [164], bridging human intent with response devices. Thanks to their ultrathin geometry, mechanical flexibility, high pressure sensitivity, and fine spatial resolution, flexible pressure sensors can be seamlessly integrated into smart wearables, such as gloves, sleeves, and textile patches [151, 165]. For instance, smart gloves embedded with high-density pressure arrays can accurately capture finger flexion, palm gestures, and force distributions across the hand, allowing precise control of virtual avatars, robotic manipulators (Figure 11b), or immersive virtual/augmented reality (VR/AR) interfaces in real-time with minimal latency [151, 166–167]. Their conformability ensures intimate skin contact, enabling the detection of fine kinematic nuances, such as wrist tilt, finger splay, for gesture recognition and tactile command input [62] (Figure 11c). Beyond specialized handwear, flexible pressure sensors are also driving innovation across broader HMI applications. In wearable technology, these sensors can be discreetly embedded into clothing or accessories to monitor joint movements, posture changes, or intentional pressure inputs, facilitating hands-free control of electronic devices and smart home systems [168–169]. Within intelligent environments, flexible pressure sensors can be integrated into furniture, flooring, or architectural surfaces to perceive user presence, location, and activity, enabling automated, personalized environmental control such as adaptive lighting, temperature regulation, or media playback [170].

Moreover, their potential extends to medical and assistive applications, including limb pressure monitoring for rehabilitation or as non-invasive HMI interfaces for individuals with limited mobility, empowering independent communication and interaction with their surroundings [161, 171]. The combination of high sensitivity, seamless integration, and biocompatibility positions these sensors as a cornerstone technology for next-generation HMIs, promising more natural, personalized, and efficient human–computer interaction experiences.

5.3 | Soft Robotics

In the rapidly evolving field of soft robotics and human–robot interaction (HRI), flexible pressure sensors serve as core

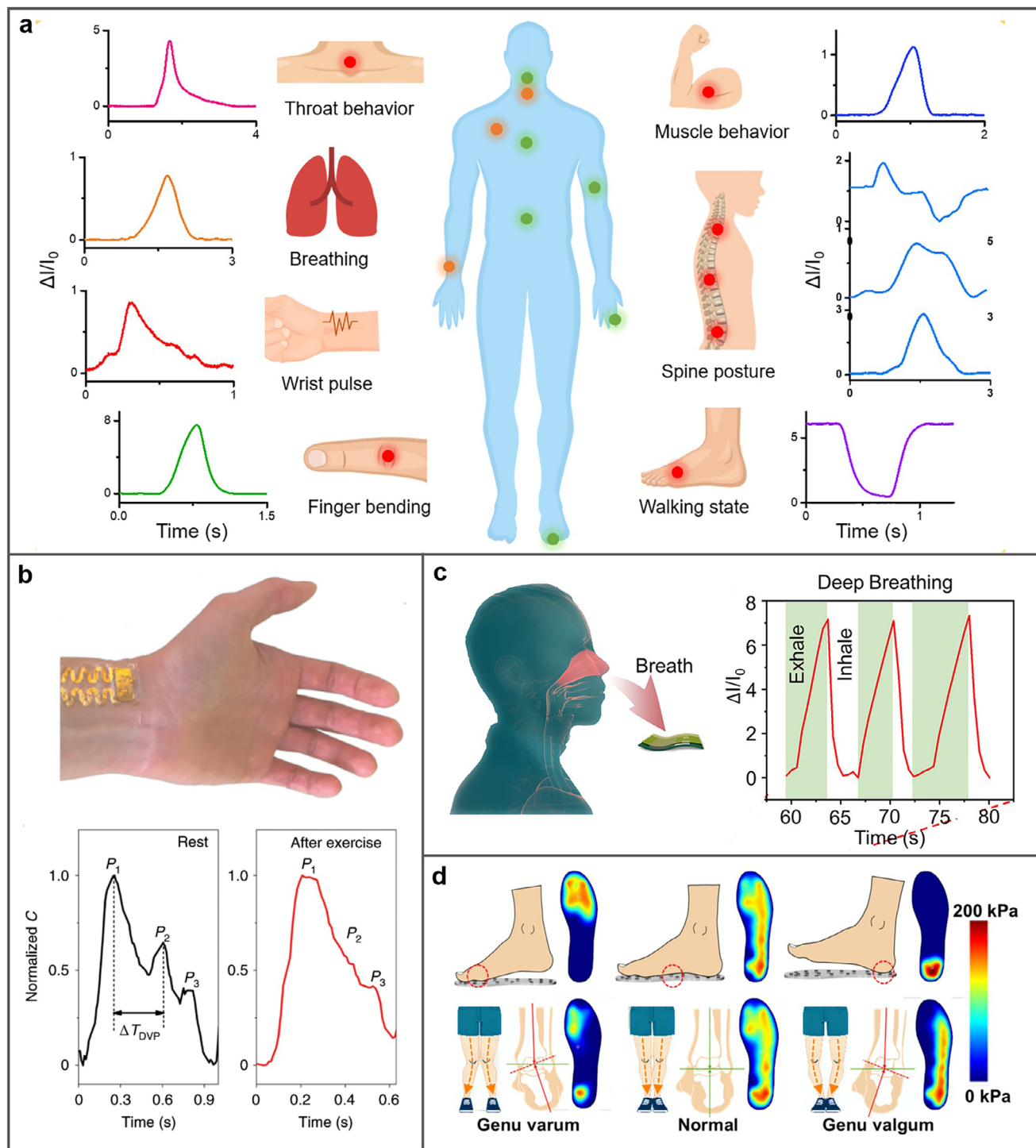


FIGURE 10 | Applications for health monitoring. (a) Schematic illustration of flexible sensors integrated on different positions of the human body with corresponding electric signals, including the throat, chest, and wrist for physiological signals and the finger, arm, spine, and foot for motion signals. Reproduced with permission [83]. Copyright 2021, American Chemical Society. (b) Photograph of the pressure sensor attached near the wrist artery (top). Real-time enlarged-view pulse wave monitoring of a human subject before and after 3 min of exercise (bottom). Reproduced with permission [152]. Copyright 2020, Springer Nature. (c) A pressure sensor integrated into a respiratory monitoring system for detecting exhalation and inhalation cycles. Reproduced with permission [156]. Copyright 2021, American Chemical Society. (d) Schematic diagrams and plantar pressure distributions for toe, midfoot, and heel contact (top); foot skeletal structure and plantar pressure distributions for normal stance, genu varum, and genu valgum stances (bottom). Reproduced with permission [27]. Copyright 2025, The American Association for the Advancement of Science.

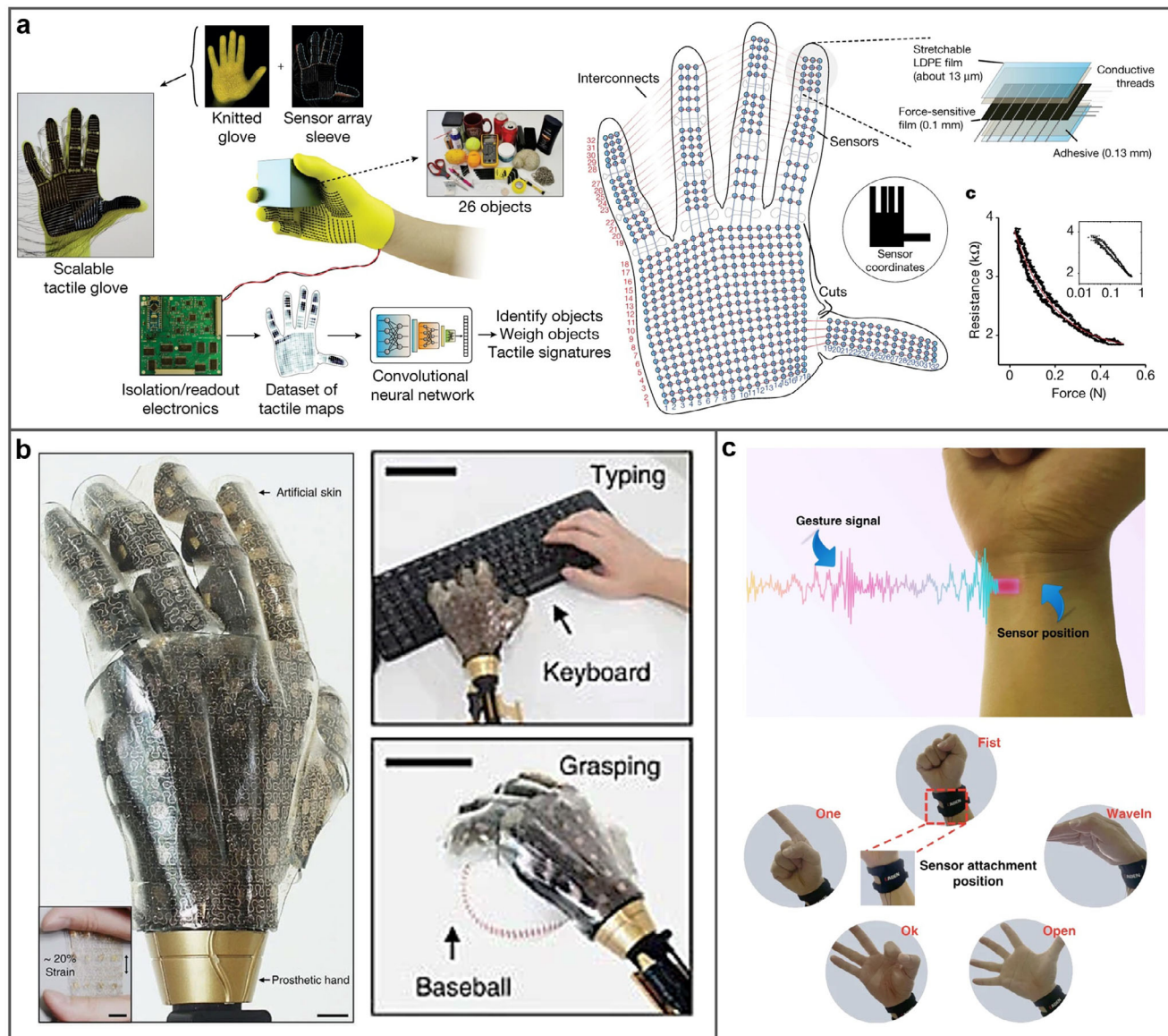


FIGURE 11 | Applications in human–machine interfaces. (a) A sensor array integrated into a custom-knit glove, covering the entire hand to enable object recognition and investigation of tactile signatures during human grasping. Reproduced with permission [151]. Copyright 2019, The Authors, published by Springer Nature. (b) Smart artificial skin embedded with stretchable sensors mounted on a prosthetic hand, capable of recording temporal resistance changes during tapping and grasping actions. Scale bars: 1 cm in the left panel, 10 cm in the top right panel, and 5 cm in the bottom right panel. Reproduced with permission [167]. Copyright 2014, Springer Nature. (c) A wearable sensor attached to the wrist for recognizing different gesture signals. Reproduced with permission [62]. Copyright 2023, The Authors, published by Springer Nature.

components of e-skin systems (Figure 12a), enabling robots to perceive and respond to physical stimuli in a human-like manner [150]. When deployed in large-area, conformable arrays across robotic surfaces, such as grippers, fingers (Figure 12b,c), arms, or full exoskeletons, these sensors provide continuous monitoring of contact forces (Figure 12d), pressure distributions, and object interaction dynamics [25, 150, 172]. The tactile feedback afforded by these sensors is crucial for dexterous and adaptive manipulation. For instance, robotic grippers equipped with high-sensitivity pressure sensors can detect incipient slippage, dynamically adjust grip force, and even differentiate object textures or shapes based on subtle force signatures. Such capabilities are essential for handling fragile, deformable, or irregularly shaped objects in unstructured environments [25,

34, 173]. The combination of mechanical flexibility, scalability for large-area fabrication (e.g., via printing techniques), high sensitivity across wide pressure ranges, and enhanced durability makes engineered pressure sensors ideal for realizing advanced e-skins that bridge the gap between rigid, insensate machines and the adaptive interaction capabilities of biological organisms [174–175]. These e-skins not only provide robust tactile sensing but also support integration with multimodal sensing platforms, combining pressure with temperature, humidity, and proximity detection. Additional functionalities, including on-skin signal processing, wireless communication, and self-healing capabilities, further enhance the autonomy and practicality of soft robotics in diverse applications [176–177].

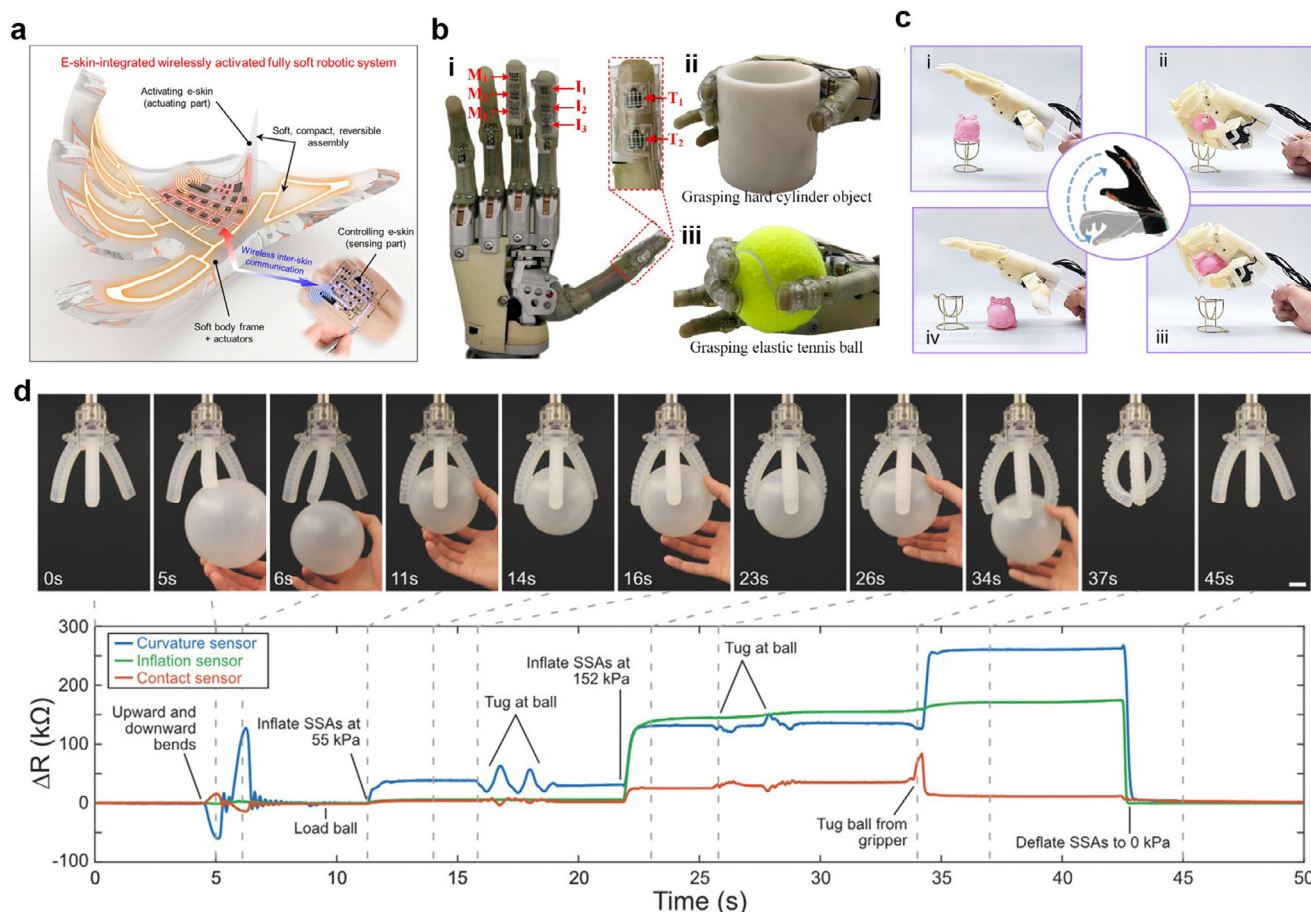


FIGURE 12 | Applications in soft robotics and electronic skins. (a) A fully soft robot wirelessly activated and capable of communicating with e-skin worn by a human user. Reproduced with permission [150]. Copyright 2018, The American Association for the Advancement of Science. (b) A humanoid robotic hand integrated with tactile sensors, capable of grasping both a rigid cylindrical object and an elastic tennis ball. Reproduced under terms of the CC-BY license [172]. Copyright 2022, The Authors. (c) A smart glove system that records and processes joint bending signals in real time, enabling precise manipulator control for object grasping. Reproduced with permission [166]. Copyright 2021, Published by Elsevier B.V. (d) A soft robotic gripper equipped with sensors on three fingers, showing both images of object manipulation and a corresponding time-resolved plot of ΔR recorded from all sensors. Scale bar is 20 mm. Reproduced with permission [178]. Copyright 2018, Wiley-VCH Verlag GmbH & Co.

6 | Conclusion, Challenges, and Future Perspectives

6.1 | Conclusion

This review provides a detailed assessment of the design principles, fundamental mechanisms, and application pathways which are required toward the engineering of high-performance flexible piezoresistive pressure sensors. The core functionality of these devices originates from the interplay of three physical phenomena: pressure-modulated contact resistance, quantum tunneling across nanogaps, and dynamic reconfiguration of conductive percolation networks. Mastery of these mechanisms provides the essential foundation for rational sensor design.

Building upon this foundation, we detailed a structured framework for sensor evaluation based on a suite of key performance metrics, including sensitivity, LoD, linearity, response time, hysteresis, and long-term durability. To this end, we have systematically categorized and explored a comprehensive toolbox of

advanced performance enhancement strategies. These strategies were broadly divided into two synergistic domains: materials engineering, which compositional and chemical innovations like hybrid composites, surface functionalization, porosity engineering, and graded conductive multilayers; and structural designs, which employs physical and architectural ingenuity through surface microstructuring, hierarchical layering, and the creation of complex three-dimensional architectures.

These coordinated advances have enabled transformative applications in continuous health monitoring, intuitive human-machine interfaces, and dexterous soft robotics. Overall, this review maps the trajectory from fundamental physical transduction mechanisms to macroscopic performance metrics and subsequently to targeted material and structural design strategies, thereby providing a roadmap for rational sensor development. A central perspective emerging from this framework is that realizing next-generation flexible electronics relies less on the isolated discovery of a “single magic material” and more on a holistic, multidisciplinary paradigm that co-optimizes materials chem-

istry, multiscale structural architectures, and device mechanics to meet the multifaceted demands of real-world applications.

6.2 | Challenges

Although this review highlights notable progress, widespread implementation of advanced, intelligent, and autonomous flexible piezoresistive sensors continues to face several recurring challenges that also define key opportunities.

To surpass the current performance limitations, future research must explore beyond conventional material choices and established novel sensing principles. Emerging 2D materials beyond graphene, such as MXenes, transition metal dichalcogenides (TMDs), and hexagonal boron nitride (hBN) offer a unique portfolio of mechanical, electrical, or chemical properties that could address specific performance gaps, as shown in Figure 13a. Greater innovation will arise from multi-material combinations, using vertical stacking, lateral heterojunctions, and hierarchical composites to create hybrid architectures with synergistic properties unattainable in single-component systems. In parallel, molecular-level design through covalent grafting of mechano-responsive polymers or supramolecular assembly can yield sensors with programmable sensitivity profiles, ultra-fast response, and minimal hysteresis. Integrating self-healing nanocomposites will further improve device durability.

Advancing from single-parameter detection, future systems will achieve monolithic multimodal sensing on a single flexible substrate, as illustrated in Figure 13b. By exploiting the versatile surface chemistry of materials like graphene derivatives, one can co-integrate physical sensors (for pressure, temperature, and humidity) with biopotential electrodes (for ECG) and chemo-responsive interfaces (for sweat biomarkers such as lactate, glucose, cortisol). However, such monolithic integration inevitably raises the critical issue of cross-talk, because multiple stimuli and deformation modes can simultaneously perturb shared conductive pathways and interfaces. Therefore, next-generation multimodal platforms should incorporate decoupling-by-design and decoupling-by-algorithm strategies, including asymmetric/differential electrode layouts, rigid-island or mechanically isolated architectures, reference channels/arrays for common-mode rejection, and machine-learning-assisted signal separation when multichannel outputs are available [179–180]. These advances will enable a comprehensive, real-time snapshot of wearer's physiological and metabolic state, moving wearable technology toward truly personalized medicine.

Despite rapid progress, direct comparison across literatures remains challenging because key performance metrics are often measured under nonuniform conditions. Variations in calibration procedures, loading geometry/contact area, pressure waveform and loading rate, as well as environmental factors (temperature/humidity), can significantly influence extracted figures of merit such as sensitivity, LoD, hysteresis, response/recovery time, durability, and baseline drift. In addition, systematic evaluations under different calibration and conditioning methods highlight that repeatability, drift, hysteresis, and accuracy can be strongly method-dependent [181], reinforcing the need for harmonized practices. Looking forward, establishing broadly accepted com-

munity guidelines, including (i) unified metric definitions and calculation methods, (ii) recommended calibration routines and reference loads, (iii) standardized loading profiles (static/step, cyclic, and application-relevant waveforms), (iv) environmental conditioning and reporting, and (v) minimum reporting templates for durability and drift tests, would greatly improve reproducibility, enable fair benchmarking, and accelerate translation from proof-of-concept demonstrations to reliable wearable products.

6.3 | Future Perspectives

The foundational work on materials and structural engineering has set the stage for the next great leap: the transition from single-modality components to fully integrated, intelligent, and autonomous perceptual systems. Building upon the current state-of-the-art, several interconnected research directions are poised to define the future of this field.

A transition from passive sensing to neuromorphic in-sensor computing is crucial for addressing the data bottleneck associated with high-density arrays and for replicating the efficiency observed in biological perception. Embedding artificial synaptic elements like memristive devices, ferroelectric transistors, or electrolyte-gated transistors (as shown in Figure 13d), directly into the sensor matrix could allow simultaneous perception, computation, and memory functions [182–184]. Such “neuromorphic mechanoreceptors” could conduct complex tasks like signal filtering, feature extraction, and pattern recognition directly at the sensing interface. This would radically reduce data transmission overhead, latency, and power consumption, enabling distributed, event-driven tactile intelligence. Such capabilities are critically needed for the next generation of intelligent prosthetics, responsive robotic skin, and real-time decision-making in edge computing devices.

The interconnect complexity of dense electrode arrays presents a primary barrier to scaling electronic skin (e-skin). Alternative readout strategies, such as electrical impedance tomography (EIT), circumvent this by eliminating the need for direct pixel-electrode connections, as demonstrated in Figure 13c. EIT enables spatially resolved pressure mapping by injecting current and measuring voltage between various electrode pairs in a cyclic sequence, sophisticated algorithms can reconstruct a high-resolution 2D conductivity (and thus pressure) distribution across a continuous sensing film. This approach enables large-area, high-resolution tactile surfaces with minimal wiring, and enhanced mechanical durability. Systems employing EIT can achieve high tactile acuity, resolving not only pressure magnitude and gradient but also texture and incipient slip, which are all crucial for next-generation robotic manipulation and closed-loop prosthetic feedback systems.

To fully unlock the value hidden within the rich, multi-dimensional data streams generated by these advanced sensors, the deep integration of machine learning and deep learning models is not just an option, but a necessity. Convolutional neural networks can be applied to spatial sensor data for advanced tactile imaging and object recognition. In parallel, recurrent neural networks and long short-term memory architectures are perfectly

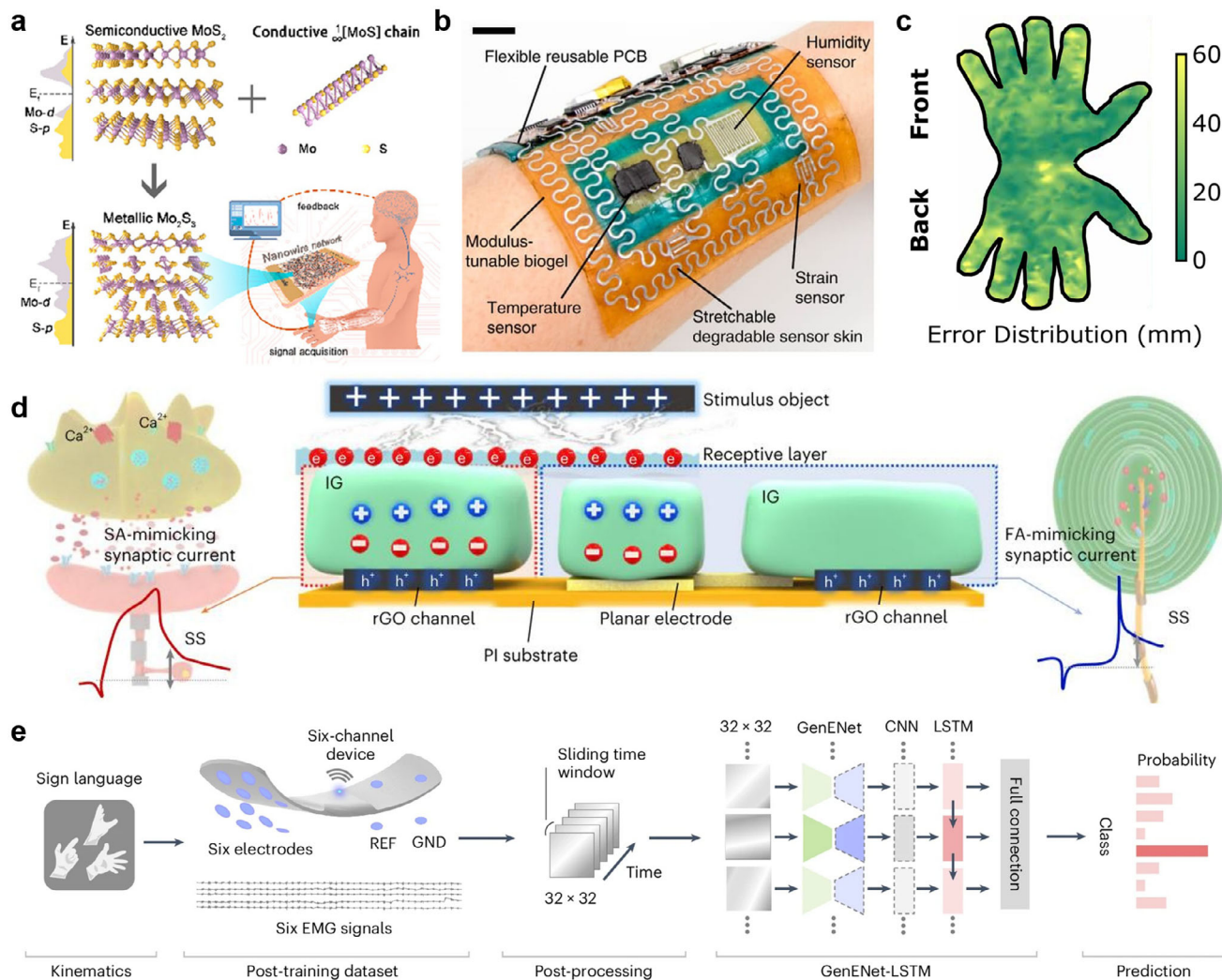


FIGURE 13 | Summary of key remaining challenges and actionable future directions for flexible piezoresistive pressure sensors. (a) Next-generation sensing materials and structural designs to overcome performance trade-offs. Reproduced with permission [16]. Copyright 2023, American Chemical Society. (b) monolithic multi-modal sensing platform with decoupling strategies to suppress cross-talk. Scale bar: 3 cm. Reproduced with permission [5]. Copyright 2020, The Author(s), published by Springer Nature. (c) Electrical impedance tomography (EIT)-based high-resolution pressure mapping that reduces interconnect complexity for large-area e-skins. Reproduced with permission [185]. Copyright 2025, The American Association for the Advancement of Science. (d) Neuromorphic mechanoreceptors-inspired in-sensor computing for low-power, low-latency tactile intelligence. Reproduced with permission [182]. Copyright 2025, The Author(s), published by Springer Nature. (e) Deep-learning-assisted signal decoupling and prediction for robust operation under unconstrained real-world conditions. Reproduced with permission [186]. Copyright 2025, The Author(s), published by Springer Nature.

suites to process temporal physiological signals for dynamic event detection. These AI models can enable the accurate, real-time classification of complex hand gestures, subtle changes in gait, or early indicators of health anomalies, as shown in Figure 13d. Future wearable pressure sensing systems are expected to increasingly rely on co-designed mechanical architectures and data-driven algorithms to decouple pressure from motion-induced artifacts (stretching/bending), thereby improving accuracy and robustness in unconstrained daily-life conditions [187–188]. Looking further ahead, with sufficient longitudinal data collection, predictive analytics models could be trained to detect long-term trends and forecast critical health events, heralding a monumental shift from reactive to truly preventative and personalized healthcare.

From a commercialization perspective, manufacturability, including throughput, yield, reproducibility, and packaging/interconnect complexity, will ultimately determine whether high-performance devices can translate beyond laboratory demonstrations. Although complex 3D micro/porous architectures provide strong performance, their scale-up is frequently limited by batch-to-batch uniformity and robust interconnect integration. Scalable alternatives include reusable replica molding/templating and printing-enabled fabrication of 3D microstructures, both of which can be adapted toward large-area manufacturing and roll-to-roll-compatible processing when materials and curing budgets permit. Regarding CMOS compatibility, CMOS-MEMS and advanced MEMS pressure-sensor integration illustrate established co-integration routes,

but soft polymer-based 3D architectures typically require hybrid integration [13, 189] (separate fabrication followed by transfer/assembly) to satisfy temperature/material compatibility and packaging stability requirements.

By vigorously pursuing these future directions, flexible piezoresistive sensing can evolve beyond discrete components toward unified intelligent platforms that couple materials, mechanics, electronics, and computation, enabling advances in wearable healthcare, human-machine interfaces, soft robotics, and ubiquitous intelligent sensing.

Acknowledgements

This work was supported by the European Union through the Horizon Europe research and innovation program HYPERSONIC (GA-101129613) as well as the Agence Nationale de la Recherche through the Interdisciplinary Thematic Institute SysChem via the IdEx Unistra (ANR-10-IDEX-0002) within the program Investissement d'Avenir, the Foundation Jean-Marie Lehn, the Institut Universitaire de France (IUF) and the Chinese Scholarship Council.

Open access publication funding provided by COUPERIN CY26.

Conflicts of Interest

The authors declare no conflicts of interests.

Data Availability Statement

The data that support the findings of this study are available from the corresponding author upon reasonable request.

References

1. J. Park, Y. Lee, S. Cho, et al., "Soft Sensors and Actuators for Wearable Human-Machine Interfaces," *Chemical Reviews* 124 (2024): 1464–1534, <https://doi.org/10.1021/acs.chemrev.3c00356>.
2. X. Fu, W. Cheng, G. Wan, Z. Yang, and B. C. K. Tee, "Toward an AI Era: Advances in Electronic Skins," *Chemical Reviews* 124 (2024): 9899–9948, <https://doi.org/10.1021/acs.chemrev.4c00049>.
3. Y. Zhang, X. T. Zheng, X. Zhang, J. Pan, and A. V. Thean, "Hybrid Integration of Wearable Devices for Physiological Monitoring," *Chemical Reviews* 124 (2024): 10386–10434, <https://doi.org/10.1021/acs.chemrev.3c00471>.
4. H. C. Ates, P. Q. Nguyen, L. Gonzalez-Macia, et al., "End-to-End Design of Wearable Sensors," *Nature Reviews Materials* 7 (2022): 887–907, <https://doi.org/10.1038/s41578-022-00460-x>.
5. M. Baumgartner, F. Hartmann, M. Drack, et al., "Resilient yet Entirely Degradable Gelatin-Based Biogels for Soft Robots and Electronics," *Nature Materials* 19 (2020): 1102–1109, <https://doi.org/10.1038/s41563-020-0699-3>.
6. H. Li, P. Tan, Y. Rao, et al., "E-Tattoos: Toward Functional but Imperceptible Interfacing with Human Skin," *Chemical Reviews* 124 (2024): 3220–3283, <https://doi.org/10.1021/acs.chemrev.3c00626>.
7. S. Y. Liu, Y. F. Rao, H. Jang, P. Tan, and N. S. Lu, "Strategies for Body-conformable Electronics," *Matter* 5 (2022): 1104–1136, <https://doi.org/10.1016/j.matt.2022.02.006>.
8. Z. Shi, L. Meng, X. Shi, et al., "Morphological Engineering of Sensing Materials for Flexible Pressure Sensors and Artificial Intelligence Applications," *Nano-Micro Letters* 14 (2022): 141, <https://doi.org/10.1007/s40820-022-00874-w>.

9. Z. Nie, J. W. Kwak, M. Han, and J. A. Rogers, "Mechanically Active Materials and Devices for Bio-Interfaced Pressure Sensors—A Review," *Advanced Materials* 36 (2024): 2205609, <https://doi.org/10.1002/adma.202205609>.
10. J. Qin, L. J. Yin, Y. N. Hao, et al., "Flexible and Stretchable Capacitive Sensors with Different Microstructures," *Advanced Materials* 33 (2021): 2008267, <https://doi.org/10.1002/adma.202008267>.
11. Z. Wang, S. Guo, H. Li, et al., "The Semiconductor/Conductor Interface Piezoresistive Effect in an Organic Transistor for Highly Sensitive Pressure Sensors," *Advanced Materials* 31 (2019): 1805630, <https://doi.org/10.1002/adma.201805630>.
12. F. Yu, Q. Liu, X. Gan, et al., "Ultrasensitive Pressure Detection of Few-Layer MoS₂," *Advanced Materials* 29 (2017): 1603266, <https://doi.org/10.1002/adma.201603266>.
13. B. Huang, Y. Yu, F. Zhang, et al., "Mechanically Gated Transistor," *Advanced Materials* 35 (2023): 2305766, <https://doi.org/10.1002/adma.202305766>.
14. X. Wang, Z. Liu, and T. Zhang, "Flexible Sensing Electronics for Wearable/Attachable Health Monitoring," *Small* 13 (2017): 1602790, <https://doi.org/10.1002/smll.201602790>.
15. S. W. Kim, J. H. Lee, H. J. Ko, et al., "Mechanically Robust and Linearly Sensitive Soft Piezoresistive Pressure Sensor for a Wearable Human-Robot Interaction System," *ACS Nano* 18 (2024): 3151–3160, <https://doi.org/10.1021/acsnano.3c09016>.
16. C. Zhao, Y. Fang, H. Chen, et al., "Ultrathin Mo₂S₃ Nanowire Network for High-Sensitivity Breathable Piezoresistive Electronic Skins," *ACS Nano* 17 (2023): 4862–4870, <https://doi.org/10.1021/acsnano.2c11564>.
17. L. Pan, A. Chortos, G. Yu, et al., "An Ultra-sensitive Resistive Pressure Sensor Based on Hollow-sphere Microstructure Induced Elasticity in Conducting Polymer Film," *Nature Communications* 5 (2014): 3002, <https://doi.org/10.1038/ncomms4002>.
18. L. Shi, Z. Li, M. Chen, Y. Qin, Y. Jiang, and L. Wu, "Quantum Effect-based Flexible and Transparent Pressure Sensors with Ultrahigh Sensitivity and Sensing Density," *Nature Communications* 11 (2020): 3529, <https://doi.org/10.1038/s41467-020-17298-y>.
19. S. Min, D. H. Kim, D. J. Joe, et al., "Clinical Validation of a Wearable Piezoelectric Blood-Pressure Sensor for Continuous Health Monitoring," *Advanced Materials* 35 (2023): 2301627, <https://doi.org/10.1002/adma.202301627>.
20. L. Xie, H. Lei, Y. Liu, et al., "Ultrasensitive Wearable Pressure Sensors with Stress-Concentrated Tip-Array Design for Long-Term Bimodal Identification," *Advanced Materials* 36 (2024): 2406235, <https://doi.org/10.1002/adma.202406235>.
21. J. S. Yang, M. K. Chung, J. Y. Yoo, et al., "Interference-free Nanogap Pressure Sensor Array with High Spatial Resolution for Wireless Human-Machine Interfaces Applications," *Nature Communications* 16 (2025): 2024, <https://doi.org/10.1038/s41467-025-57232-8>.
22. H. Niu, H. Li, S. Gao, et al., "Perception-to-Cognition Tactile Sensing Based on Artificial-Intelligence-Motivated Human Full-Skin Bionic Electronic Skin," *Advanced Materials* 34 (2022): 2202622, <https://doi.org/10.1002/adma.202202622>.
23. B. Ji, Q. Zhou, B. Hu, J. Zhong, J. Zhou, and B. Zhou, "Bio-Inspired Hybrid Dielectric for Capacitive and Triboelectric Tactile Sensors with High Sensitivity and Ultrawide Linearity Range," *Advanced Materials* 33 (2021): 2100859, <https://doi.org/10.1002/adma.202100859>.
24. X. Wei, H. Li, W. J. Yue, et al., "A High-Accuracy, Real-Time, Intelligent Material Perception System with a Machine-Learning-Motivated Pressure-sensitive Electronic Skin," *Matter* 5 (2022): 1481, <https://doi.org/10.1016/j.matt.2022.02.016>.
25. R. Chen, T. Luo, J. Wang, et al., "Nonlinearity Synergy: an Elegant Strategy for Realizing High-Sensitivity and Wide-Linear-Range Pressure Sensing," *Nature Communications* 14 (2023): 6641, <https://doi.org/10.1038/s41467-023-42361-9>.

26. W. Zhu, Y. Zhuang, J. Weng, et al., "Evolution of Naturally Dried MXene-Based Composite Aerogels with Flash Joule Annealing for Large-Scale Production of Highly Sensitive Customized Sensors," *Advanced Materials* 36 (2024): 2407138, <https://doi.org/10.1002/adma.202407138>.
27. Q. Wang, H. Guan, C. Wang, et al., "A Wireless, Self-powered Smart Insole for Gait Monitoring and Recognition via Nonlinear Synergistic Pressure Sensing," *Science Advances* 11 (2025): adu1598, <https://doi.org/10.1126/sciadv.adu1598>.
28. Y. Lee, J. Myoung, S. Cho, et al., "Bioinspired Gradient Conductivity and Stiffness for Ultrasensitive Electronic Skins," *ACS Nano* 15 (2021): 1795–1804, <https://doi.org/10.1021/acsnano.0c09581>.
29. S. Lee, S. H. Byun, C. Y. Kim, et al., "Beyond Human Touch Perception: An Adaptive Robotic Skin Based on Gallium Microgranules for Pressure Sensory Augmentation," *Advanced Materials* 34 (2022): 2204805, <https://doi.org/10.1002/adma.202204805>.
30. X. Xu and B. Yan, "Bioinspired Luminescent HOF-Based Foam as Ultrafast and Ultrasensitive Pressure and Acoustic Bimodal Sensor for Human–Machine Interactive Object and Information Recognition," *Advanced Materials* 35 (2023): 2303410, <https://doi.org/10.1002/adma.202303410>.
31. C. Jeong, J. S. Lee, B. Park, C. S. Hong, J. U. Kim, and T. I. Kim, "Controllable Configuration of Sensing Band in a Pressure Sensor by Lenticular Pattern Deformation on Designated Electrodes," *Advanced Materials* 31 (2019): 1902689, <https://doi.org/10.1002/adma.201902689>.
32. X. Z. Lin, Y. Teng, H. Xue, et al., "Janus Conductive Mechanism: An Innovative Strategy Enabling Ultra-Wide Linearity Range Pressure Sensing for Multi-Scenario Applications," *Advanced Functional Materials* 34 (2024): 2316314, <https://doi.org/10.1002/adfm.202316314>.
33. E. Su, F. Wu, S. Zhao, Y. Li, and C. Deng, "Layered MXene/Aramid Composite Film for a Soft and Sensitive Pressure Sensor," *ACS Applied Materials & Interfaces* 14 (2022): 15849–15858, <https://doi.org/10.1021/acami.2c01914>.
34. Y. He, Y. Cheng, C. Yang, and C. F. Guo, "Creep-free Polyelectrolyte Elastomer for Drift-free Iontronic Sensing," *Nature Materials* 23 (2024): 1107–1114, <https://doi.org/10.1038/s41563-024-01848-6>.
35. R. Qin, J. Nong, K. Wang, et al., "Recent Advances in Flexible Pressure Sensors Based on MXene Materials," *Advanced Materials* 36 (2024): 2312761, <https://doi.org/10.1002/adma.202312761>.
36. N. Li, H. Li, J. H. Feng, et al., "Microstructure-Modulated Linear-Response Flexible Pressure Sensors," *Advanced Functional Materials* 36 (2025): 09776, <https://doi.org/10.1002/adfm.202509776>.
37. S. R. A. Ruth, V. R. Feig, H. Tran, and Z. N. Bao, "Microengineering Pressure Sensor Active Layers for Improved Performance," *Advanced Functional Materials* 30 (2020): 2003491, <https://doi.org/10.1002/adfm.202003491>.
38. X. Cui, F. Huang, X. Zhang, et al., "Flexible Pressure Sensors via Engineering Microstructures for Wearable Human-Machine Interaction and Health Monitoring Applications," *Iscience* 25 (2022): 104148, <https://doi.org/10.1016/j.isci.2022.104148>.
39. G. F. Sun, P. Wang, Y. X. Jiang, H. C. Sun, C. Z. Meng, and S. J. Guo, "Recent Advances in Flexible and Soft Gel-Based Pressure Sensors," *Soft Science* 2 (2022): 17, <https://doi.org/10.20517/ss.2022.16>.
40. J. F. Zhu, C. J. Zhou, and M. Zhang, "Recent Progress in Flexible Tactile Sensor Systems: From Design to Application," *Soft Science* 1 (2021): 3.
41. J. J. Yu, K. Zhang, and Y. Deng, "Recent Progress in Pressure and Temperature Tactile Sensors: Principle, Classification, Integration and Outlook," *Soft Science* 1 (2021): 6.
42. Y. Luo, M. R. Abidian, J. H. Ahn, et al., "Technology Roadmap for Flexible Sensors," *ACS Nano* 17 (2023): 5211–5295, <https://doi.org/10.1021/acsnano.2c12606>.
43. C. Z. Zhao, J. Park, S. E. Root, and Z. N. Bao, "Skin-Inspired Soft Bioelectronic Materials, Devices and Systems," *Nature Reviews Bioengineering* 2 (2024): 671–690, <https://doi.org/10.1038/s44222-024-00194-1>.
44. Z. Zhang, Q. Liu, H. L. Ma, et al., "Recent Advances in Graphene-Based Pressure Sensors: A Review," *IEEE Sensors Journal* 24 (2024): 25227–25248, <https://doi.org/10.1109/JSEN.2024.3419243>.
45. Y. Jin, S. Xue, and Y. He, "Flexible Pressure Sensors Enhanced by 3D-Printed Microstructures," *Advanced Materials* 37 (2025): 2500076, <https://doi.org/10.1002/adma.202500076>.
46. R. Holm, *Electric Contacts: Theory and Application* (Springer Science & Business Media, 2013).
47. Y. Pang, K. Zhang, Z. Yang, et al., "Epidermis Microstructure Inspired Graphene Pressure Sensor with Random Distributed Spinosum for High Sensitivity and Large Linearity," *ACS Nano* 12 (2018): 2346–2354, <https://doi.org/10.1021/acsnano.7b07613>.
48. J. Park, Y. Lee, J. Hong, et al., "Tactile-Direction-Sensitive and Stretchable Electronic Skins Based on Human-Skin-Inspired Interlocked Microstructures," *ACS Nano* 8 (2014): 12020–12029, <https://doi.org/10.1021/nn505953t>.
49. T. An, Y. Zhang, J. Wen, et al., "Multi-Level Pyramidal Microstructure-Based Pressure Sensors with High Sensitivity and Wide Linear Range for Healthcare Monitoring," *ACS Sensors* 9 (2024): 726–735, <https://doi.org/10.1021/acssensors.3c02001>.
50. N. Li, S. Gao, Y. Li, J. W. Liu, W. H. Song, and G. Z. Shen, "Multi-attribute Wearable Pressure Sensor Based on Multilayered Modulation with High Constant Sensitivity over a Wide Range," *Nano Research* 16 (2023): 7583–7592, <https://doi.org/10.1007/s12274-022-5371-6>.
51. S. Pyo, J. Lee, W. Kim, E. Jo, and J. Kim, "Multi-Layered, Hierarchical Fabric-Based Tactile Sensors with High Sensitivity and Linearity in Ultrawide Pressure Range," *Advanced Functional Materials* 29 (2019): 1902484, <https://doi.org/10.1002/adfm.201902484>.
52. J. Chen, K. Chen, J. Jin, et al., "Outstanding Synergy of Sensitivity and Linear Range Enabled by Multigradient Architectures," *Nano Letters* 23 (2023): 11958–11967, <https://doi.org/10.1021/acs.nanolett.3c04204>.
53. C. Muhammed Ajmal, S. Cha, W. Kim, K. P. Faseela, H. Yang, and S. Baik, "Invariable Resistance of Conductive Nanocomposite over 30% Strain," *Science Advances* 8 (2022): abn3365, <https://doi.org/10.1126/sciadv.abn3365>.
54. S. Q. Ding, B. G. Han, X. F. Dong, et al., "Pressure-Sensitive Behaviors, Mechanisms and Model of Field Assisted Quantum Tunneling Composites," *Polymer* 113 (2017): 105–118, <https://doi.org/10.1016/j.polymer.2017.02.058>.
55. S. Stassi, V. Cauda, G. Canavese, and C. F. Pirri, "Flexible Tactile Sensing Based on Piezoresistive Composites: A Review," *Sensors* 14 (2014): 5296–5332, <https://doi.org/10.3390/s140305296>.
56. D. Lee, H. Lee, Y. Jeong, Y. Ahn, G. Nam, and Y. Lee, "Highly Sensitive, Transparent, and Durable Pressure Sensors Based on Sea-Urchin Shaped Metal Nanoparticles," *Advanced Materials* 28 (2016): 9364–9369, <https://doi.org/10.1002/adma.201603526>.
57. J. Park, Y. Lee, J. Hong, et al., "Giant Tunneling Piezoresistance of Composite Elastomers with Interlocked Microdome Arrays for Ultrasensitive and Multimodal Electronic Skins," *ACS Nano* 8 (2014): 4689–4697, <https://doi.org/10.1021/nn500441k>.
58. C. B. Huang, S. Witomska, A. Aliprandi, et al., "Molecule–Graphene Hybrid Materials with Tunable Mechanoreponse: Highly Sensitive Pressure Sensors for Health Monitoring," *Advanced Materials* 31 (2019): 1804600, <https://doi.org/10.1002/adma.201804600>.
59. A. Alidoust, M. Haghgoo, R. Ansari, M. K. H. Aghdam, and S. H. Jang, "A Finite Element Percolation Tunneling Approach on the Electrical Properties of Carbon Nanotube Elastomer Nanocomposite Pressure Sensors," *Composites Part A: Applied Science and Manufacturing* 180 (2024): 108111, <https://doi.org/10.1016/j.compositesa.2024.108111>.

60. M. Wang, R. Gurunathan, K. Imasato, et al., "A Percolation Model for Piezoresistivity in Conductor–Polymer Composites," *Advanced Theory and Simulations* 2 (2018): 1800125, <https://doi.org/10.1002/adts.201800125>.
61. M. Chen, W. Luo, Z. Xu, et al., "An Ultrahigh Resolution Pressure Sensor Based on Percolative Metal Nanoparticle Arrays," *Nature Communications* 10 (2019): 4024, <https://doi.org/10.1038/s41467-019-12030-x>.
62. Z. Xu, D. Wu, Z. Chen, et al., "A Flexible Pressure Sensor with Highly Customizable Sensitivity and Linearity via Positive Design of Microhierarchical Structures with a Hyperelastic Model," *Microsystems & Nanoengineering* 9 (2023): 5, <https://doi.org/10.1038/s41378-022-00477-w>.
63. Y. Lee, J. Park, S. Cho, et al., "Flexible Ferroelectric Sensors with Ultrahigh Pressure Sensitivity and Linear Response over Exceptionally Broad Pressure Range," *ACS Nano* 12 (2018): 4045–4054, <https://doi.org/10.1021/acsnano.8b01805>.
64. W. Cao, Y. Luo, Y. Dai, et al., "Piezoresistive Pressure Sensor Based on a Conductive 3D Sponge Network for Motion Sensing and Human–Machine Interface," *ACS Applied Materials & Interfaces* 15 (2023): 3131–3140, <https://doi.org/10.1021/acscami.2c18203>.
65. H. T. Chen, Z. M. Su, Y. Song, et al., "Omnidirectional Bending and Pressure Sensor Based on Stretchable CNT-PU Sponge," *Advanced Functional Materials* 27 (2017): 1604434, <https://doi.org/10.1002/adfm.201604434>.
66. M. H. Cao, J. Su, S. Q. Fan, H. W. Qiu, D. L. Su, and L. Li, "Wearable Piezoresistive Pressure Sensors Based on 3D Graphene," *Chemical Engineering Journal* 406 (2021): 126777, <https://doi.org/10.1016/j.cej.2020.126777>.
67. Y. J. Zhao, L. W. Miao, Y. Xiao, and P. Sun, "Research Progress of Flexible Piezoresistive Pressure Sensor: A Review," *IEEE Sensors Journal* 24 (2024): 31624–31644, <https://doi.org/10.1109/JSEN.2024.3443423>.
68. S. Xu, Z. Xu, D. Li, et al., "Recent Advances in Flexible Piezoresistive Arrays: Materials, Design, and Applications," *Polymers* 15 (2023): 2699, <https://doi.org/10.3390/polym15122699>.
69. Y. P. Zang, F. J. Zhang, C. A. Di, and D. B. Zhu, "Advances of Flexible Pressure Sensors toward Artificial Intelligence and Health Care Applications," *Materials Horizons* 2 (2015): 140–156, <https://doi.org/10.1039/C4MH00147H>.
70. B. Huang, J. Feng, J. He, et al., "High Sensitivity and Wide Linear Range Flexible Piezoresistive Pressure Sensor with Microspheres as Spacers for Pronunciation Recognition," *ACS Applied Materials & Interfaces* 16 (2024): 19298–19308, <https://doi.org/10.1021/acscami.4c04156>.
71. X. Wang, G. Wu, X. Zhang, et al., "Traditional Chinese Medicine (TCM)-Inspired Fully Printed Soft Pressure Sensor Array with Self-Adaptive Pressurization for Highly Reliable Individualized Long-Term Pulse Diagnostics," *Advanced Materials* 37 (2025): 2410312, <https://doi.org/10.1002/adma.202410312>.
72. S. Chen, K. Jiang, Z. Lou, D. Chen, and G. Z. Shen, "Recent Developments in Graphene-Based Tactile Sensors and E-Skins," *Advanced Materials Technologies* 3 (2018): 1700248, <https://doi.org/10.1002/admt.201700248>.
73. J. Kim, A. S. Campbell, B. E. de Avila, and J. Wang, "Wearable Biosensors for Healthcare Monitoring," *Nature Biotechnology* 37 (2019): 389–406, <https://doi.org/10.1038/s41587-019-0045-y>.
74. K. Lim, H. Seo, W. G. Chung, et al., "Material and Structural Considerations for High-Performance Electrodes for Wearable Skin Devices," *Communications Materials* 5 (2024): 49, <https://doi.org/10.1038/s43246-024-00490-8>.
75. W. Cheng, X. Wang, Z. Xiong, et al., "Frictionless Multiphase Interface for Near-ideal Aero-elastic Pressure Sensing," *Nature Materials* 22 (2023): 1352–1360, <https://doi.org/10.1038/s41563-023-01628-8>.
76. M. Z. Zeng, J. Ding, Y. Tian, et al., "Phase Separation Manipulated Gradient Conductivity for a High-Precision Flexible Pressure Sensor," *Advanced Functional Materials* 34 (2024): 2411390, <https://doi.org/10.1002/adfm.202411390>.
77. Y. Zhu, X. Hu, X. Yan, W. Ni, M. Wu, and J. Liu, "Nanoengineering Ultrathin Flexible Pressure Sensors with Superior Sensitivity and Wide Range via Nanocomposite Structures," *ACS Sensors* 9 (2024): 4176–4185, <https://doi.org/10.1021/acssensors.4c01171>.
78. Y. B. Wan, Z. G. Qiu, J. Yuan, J. L. Yang, J. Z. Li, and C. F. Guo, "A Tutorial of Characterization Methods on Flexible Pressure Sensors: Fundamental and Applications," *Journal of Physics D: Applied Physics* 57 (2024): 093002, <https://doi.org/10.1088/1361-6463/ad0e95>.
79. X. F. Wang, J. H. Yu, Y. X. Cui, and W. Li, "Research Progress of Flexible Wearable Pressure Sensors," *Sensors and Actuators A: Physical* 330 (2021): 112838, <https://doi.org/10.1016/j.sna.2021.112838>.
80. T. Q. Trung and N. E. Lee, "Flexible and Stretchable Physical Sensor Integrated Platforms for Wearable Human-Activity Monitoring and Personal Healthcare," *Advanced Materials* 28 (2016): 4338–4372, <https://doi.org/10.1002/adma.201504244>.
81. W. T. Guo, X. G. Tang, Z. Tang, and Q. J. Sun, "Recent Advances in Polymer Composites for Flexible Pressure Sensors," *Polymers* 15 (2023): 2176, <https://doi.org/10.3390/polym15092176>.
82. S. Gong, W. Schwalb, Y. Wang, et al., "A Wearable and Highly Sensitive Pressure Sensor with Ultrathin Gold Nanowires," *Nature Communications* 5 (2014): 3132, <https://doi.org/10.1038/ncomms4132>.
83. T. Yang, W. Deng, X. Chu, et al., "Hierarchically Microstructure-Bioinspired Flexible Piezoresistive Bioelectronics," *ACS Nano* 15 (2021): 11555–11563, <https://doi.org/10.1021/acsnano.1c01606>.
84. F. Zhuo, Z. Ding, X. Yang, et al., "Advanced Morphological and Material Engineering for High-Performance Interfacial Iontronic Pressure Sensors," *Advanced Science* 12 (2025): 2413141, <https://doi.org/10.1002/advs.202413141>.
85. A. Rinaldi, A. Tamburrano, M. Fortunato, and M. S. Sarto, "A Flexible and Highly Sensitive Pressure Sensor Based on a PDMS Foam Coated with Graphene Nanoplatelets," *Sensors* 16 (2016): 2148, <https://doi.org/10.3390/s16122148>.
86. H. N. Qiu, J. Lin, L. X. Hou, R. Xiao, Q. Zheng, and Z. L. Wu, "Stress Relaxation and Creep Response of Glassy Hydrogels with Dense Physical Associations," *ACS Applied Materials & Interfaces* 17 (2025): 9981–9991, <https://doi.org/10.1021/acscami.4c22398>.
87. G. Mogli, M. Costantini, and S. Stassi, "Highly Sensitive PDMS-Ag Nanoflakes Porous Pressure Sensors Prepared by Templating and Molding Approaches for Wearable Applications," *Sensors and Actuators A: Physical* 392 (2025): 116734, <https://doi.org/10.1016/j.sna.2025.116734>.
88. H. Tian, Y. Shu, X. F. Wang, et al., "A Graphene-Based Resistive Pressure Sensor with Record-High Sensitivity in a Wide Pressure Range," *Scientific Reports* 5 (2015): 8603, <https://doi.org/10.1038/srep08603>.
89. Y. Li, Y. Wei, Y. Yang, et al., "The Soft-Strain Effect Enabled High-Performance Flexible Pressure Sensor and Its Application in Monitoring Pulse Waves," *Research* 2022 (2022): 0002, <https://doi.org/10.34133/research.0002>.
90. Y. X. Qin, B. Gao, and C. Zhou, "Highly Sensitive and Breathability Flexible Piezoresistive Pressure Sensor Based on Xylon," *Advanced Materials Technologies* 9 (2024): 2400035, <https://doi.org/10.1002/admt.202400035>.
91. X. F. Liu, Y. N. Ma, X. Y. Dai, S. X. Li, B. W. Li, and X. Zhang, "Flexible Pressure Sensor Based on Pt/PI Network with High Sensitivity and High Thermal Resistance," *Chemical Engineering Journal* 494 (2024): 152996, <https://doi.org/10.1016/j.cej.2024.152996>.
92. T. Someya, Z. Bao, and G. G. Malliaras, "The Rise of Plastic Bioelectronics," *Nature* 540 (2016): 379–385, <https://doi.org/10.1038/nature21004>.
93. J. Sun, D. Zhang, R. Zhang, et al., "Novel Polyurethane Based, Fully Flexible, High-Performance Piezoresistive Sensor for Real-Time Pressure Monitoring," *ACS Applied Materials & Interfaces* 16 (2024): 25422–25431, <https://doi.org/10.1021/acscami.4c05097>.

94. J. Li, Y. L. Zhao, Y. B. Fan, J. Y. Chen, J. H. Gong, and W. J. Li, "Flexible Wearable Electronics for Enhanced Human-Computer Interaction and Virtual Reality Applications," *Nano Energy* 138 (2025): 110821, <https://doi.org/10.1016/j.nanoen.2025.110821>.
95. M. Amjadi, K. U. Kyung, I. Park, and M. Sitti, "Stretchable, Skin-Mountable, and Wearable Strain Sensors and Their Potential Applications: A Review," *Advanced Functional Materials* 26 (2016): 1678–1698, <https://doi.org/10.1002/adfm.201504755>.
96. M. L. Hammock, A. Chortos, B. C. Tee, J. B. Tok, and Z. Bao, "25th Anniversary Article: The Evolution of Electronic Skin (E-Skin): a Brief History, Design Considerations, and Recent Progress," *Advanced Materials* 25 (2013): 5997–6038, <https://doi.org/10.1002/adma.201302240>.
97. C. Wang, K. Xia, H. Wang, X. Liang, Z. Yin, and Y. Zhang, "Advanced Carbon for Flexible and Wearable Electronics," *Advanced Materials* 31 (2019): 1801072, <https://doi.org/10.1002/adma.201801072>.
98. S. Sharma, A. Chhetry, M. Sharifuzzaman, H. Yoon, and J. Y. Park, "Wearable Capacitive Pressure Sensor Based on MXene Composite Nanofibrous Scaffolds for Reliable Human Physiological Signal Acquisition," *ACS Applied Materials & Interfaces* 12 (2020): 22212–22224, <https://doi.org/10.1021/acsami.0c05819>.
99. S. Yao and Y. Zhu, "Wearable Multifunctional Sensors Using Printed Stretchable Conductors Made of Silver Nanowires," *Nanoscale* 6 (2014): 2345, <https://doi.org/10.1039/c3nr05496a>.
100. S. Xu, Y. Zhang, L. Jia, et al., "Soft Microfluidic Assemblies of Sensors, Circuits, and Radios for the Skin," *Science* 344 (2014): 70–74, <https://doi.org/10.1126/science.1250169>.
101. T. Q. Trung, S. Ramasundaram, B. U. Hwang, and N. E. Lee, "An All-Elastomeric Transparent and Stretchable Temperature Sensor for Body-Attachable Wearable Electronics," *Advanced Materials* 28 (2016): 502–509, <https://doi.org/10.1002/adma.201504441>.
102. Z. Lei, Q. Wang, S. Sun, W. Zhu, and P. Wu, "A Bioinspired Mineral Hydrogel as a Self-Healable, Mechanically Adaptable Ionic Skin for Highly Sensitive Pressure Sensing," *Advanced Materials* 29 (2017): 1700321, <https://doi.org/10.1002/adma.201700321>.
103. J. Heikenfeld, A. Jajack, J. Rogers, et al., "Wearable Sensors: Modalities, Challenges, and Prospects," *Lab on a Chip* 18 (2018): 217–248, <https://doi.org/10.1039/C7LC00914C>.
104. Q. C. Li, D. Chen, J. M. Miao, J. J. Yu, C. X. Chen, and Y. M. Liu, "Flexible Pressure Sensors Based on Reduced Graphene Oxide @ Porous Silicone Elastomers with Good Resolution and Wide Working Range," *Sensors and Actuators A: Physical* 366 (2024): 114991, <https://doi.org/10.1016/j.sna.2023.114991>.
105. F. Kang, W. Zhang, M. Liu, F. Liu, Z. Jia, and D. Jia, "Highly Flexible and Sensitive Ti₃C₂ MXene@Polyurethane Composites for Piezoresistive Pressure Sensor," *Journal of Materials Science* 57 (2022): 12894–12902, <https://doi.org/10.1007/s10853-022-07387-2>.
106. M. Beccatelli, M. Villani, F. Gentile, et al., "All-Polymeric Pressure Sensors Based on PEDOT:PSS-Modified Polyurethane Foam," *ACS Applied Polymer Materials* 3 (2021): 1563–1572, <https://doi.org/10.1021/acsapm.0c01389>.
107. X. Q. Guo, Y. F. Li, Z. R. Zeng, et al., "Ultra-sensitive Flexible Pressure Sensor with Hierarchical Structural Laser-induced Carbon Nanosheets/Carbon Nanotubes Composite Film," *Composites Science and Technology* 244 (2023): 110290, <https://doi.org/10.1016/j.compscitech.2023.110290>.
108. X. Zhang, Z. Hu, Q. Sun, et al., "Bioinspired Gradient Stretchable Aerogels for Ultrabroad-Range-Response Pressure-Sensitive Wearable Electronics and High-Efficient Separators," *Angewandte Chemie International Edition* 62 (2023): 202213952, <https://doi.org/10.1002/anie.202213952>.
109. X. Shuai, P. Zhu, W. Zeng, et al., "Highly Sensitive Flexible Pressure Sensor Based on Silver Nanowires-Embedded Polydimethylsiloxane Electrode with Microarray Structure," *ACS Applied Materials & Interfaces* 9 (2017): 26314–26324, <https://doi.org/10.1021/acsami.7b05753>.
110. Y. Cheng, M. Wang, N. Ma, et al., "Nanoscale Interlayer Engineering Enhances MXene-Based Flexible Pressure Sensor," *Nano Letters* 25 (2025): 11782–11789, <https://doi.org/10.1021/acs.nanolett.5c01464>.
111. J. Yang, C. Wang, L. Liu, H. Zhang, and J. Ma, "Water-Tolerant MXene Epidermal Sensors with High Sensitivity and Reliability for Healthcare Monitoring," *ACS Applied Materials & Interfaces* 14 (2022): 21253–21262, <https://doi.org/10.1021/acsami.2c03731>.
112. T. X. Zhang, Y. N. Zhao, Q. Long, et al., "Graphene/MXene/Cellulose Cellulosic Paper-Based Bifunctional Sensors Utilizing Molecular Bridge Strategy with Tunable Piezoresistive Effect for Temperature-Pressure Sensing," *Chemical Engineering Journal* 497 (2024): 154972, <https://doi.org/10.1016/j.cej.2024.154972>.
113. X. H. Guo, T. C. Liu, Y. M. Tang, et al., "Bioinspired Low Hysteresis Flexible Pressure Sensor Using Nanocomposites of Multiwalled Carbon Nanotubes, Silicone Rubber, and Carbon Nanofiber for Human-Computer Interaction," *ACS Applied Nano Materials* 7 (2024): 15626–15639, <https://doi.org/10.1021/acsanm.4c02631>.
114. F. Luo, A. Ciesielski, and P. Samori, "Nonlinear Conductive Graphene Composites for Pressure Sensing with a Linear Response and Voltage-Driven Thermal Correction," *Advanced Materials* 37 (2025): 2503867, <https://doi.org/10.1002/adma.202503867>.
115. H. Zhuo, Y. Hu, X. Tong, et al., "A Supercompressible, Elastic, and Bendable Carbon Aerogel with Ultrasensitive Detection Limits for Compression Strain, Pressure, and Bending Angle," *Advanced Materials* 30 (2018): 1706705, <https://doi.org/10.1002/adma.201706705>.
116. S. W. Dai, Y. L. Gu, L. Zhao, et al., "Bamboo-inspired Mechanically Flexible and Electrically Conductive Polydimethylsiloxane Foam Materials with Designed Hierarchical Pore Structures for Ultra-sensitive and Reliable Piezoresistive Pressure Sensor," *Composites Part B: Engineering* 225 (2021): 109243, <https://doi.org/10.1016/j.compositesb.2021.109243>.
117. Y. Cheng, L. Li, Z. Liu, et al., "3D Porous MXene Aerogel through Gas Foaming for Multifunctional Pressure Sensor," *Research* 2022 (2022): 9843268, <https://doi.org/10.34133/2022/9843268>.
118. S. Yang, K. Ding, W. Wang, et al., "Electrospun Fiber-Based High-Performance Flexible Multi-level Micro-structured Pressure Sensor: Design, Development and Modelling," *Chemical Engineering Journal* 431 (2022): 133700, <https://doi.org/10.1016/j.cej.2021.133700>.
119. T. Yin, Y. Cheng, Y. Hou, et al., "3D Porous Structure in MXene/PANI Foam for a High-Performance Flexible Pressure Sensor," *Small* 18 (2022): 2204806, <https://doi.org/10.1002/smll.202204806>.
120. Y. Cheng, Y. Xie, Z. Liu, et al., "Maximizing Electron Channels Enabled by MXene Aerogel for High-Performance Self-Healable Flexible Electronic Skin," *ACS Nano* 17 (2023): 1393–1402, <https://doi.org/10.1021/acsnano.2c09933>.
121. Y. Z. Du, W. X. Lu, Y. C. Liu, R. Yu, P. Z. Wu, and J. Kong, "MXene-Based Pressure Sensor with Ultrahigh Sensitivity in a Small Pressure Range for Voiceless Speaking and Abnormal Writing Recognition," *Advanced Composites and Hybrid Materials* 7 (2024): 24, <https://doi.org/10.1007/s42114-024-00838-1>.
122. M. Zhang, S. Liu, S. Liu, et al., "Multi-layered Gradient-Structured TPU/CNTs Aerogel with Ultra-wide Pressure Detection Capabilities for Machine Learning-Assisted Fruit Recognition," *Advanced Composites and Hybrid Materials* 8 (2024): 79, <https://doi.org/10.1007/s42114-024-01157-1>.
123. J. Li, N. Li, Y. Zheng, et al., "Interfacially Locked Metal Aerogel inside Porous Polymer Composite for Sensitive and Durable Flexible Piezoresistive Sensors," *Advanced Science* 9 (2022): 2201912, <https://doi.org/10.1002/advs.202201912>.
124. C. Ma, D. Xu, Y. C. Huang, et al., "Robust Flexible Pressure Sensors Made from Conductive Micropyramids for Manipulation Tasks," *ACS Nano* 14 (2020): 12866–12876, <https://doi.org/10.1021/acsnano.0c03659>.
125. J. Park, J. Kim, J. Hong, et al., "Tailoring Force Sensitivity and Selectivity by Microstructure Engineering of Multidirectional Electronic

- Skins,” *NPG Asia Materials* 10 (2018): 163–176, <https://doi.org/10.1038/s41427-018-0031-8>.
126. M. Wang, Y. Yu, Y. H. Liang, et al., “High-Performance Multilayer Flexible Piezoresistive Pressure Sensor with Bionic Hierarchical and Anisotropic Structure,” *Journal of Bionic Engineering* 19 (2022): 1439–1448, <https://doi.org/10.1007/s42235-022-00219-8>.
127. Z. Wang, L. Zhang, J. Liu, H. Jiang, and C. Li, “Flexible Hemispherical Microarrays of Highly Pressure-Sensitive Sensors Based on Breath Figure Method,” *Nanoscale* 10 (2018): 10691–10698, <https://doi.org/10.1039/C8NR01495G>.
128. J. Baek, Y. Shan, M. Mylvaganan, et al., “Mold-Free Manufacturing of Highly Sensitive and Fast-Response Pressure Sensors through High-Resolution 3D Printing and Conformal Oxidative Chemical Vapor Deposition Polymers,” *Advanced Materials* 35 (2023): 2304070, <https://doi.org/10.1002/adma.202304070>.
129. Y. Shen, Z. B. Li, Y. Xiang, J. S. Feng, X. Zhang, and T. H. Wang, “Decoupling Stretching and Sensing Regions to Achieve Strain-insensitive Iontronic Pressure Sensors for Gesture Recognition,” *Chemical Engineering Journal* 516 (2025): 163763, <https://doi.org/10.1016/j.cej.2025.163763>.
130. Y. B. Yuan, H. C. Xu, W. H. Zheng, et al., “Bending and Stretching-Insensitive, Crosstalk-Free, Flexible Pressure Sensor Arrays for Human-Machine Interactions,” *Advanced Materials Technologies* 9 (2024): 2301615, <https://doi.org/10.1002/admt.202301615>.
131. Q. Su, Q. Zou, Y. Li, et al., “A Stretchable and Strain-Unperturbed Pressure Sensor for Motion Interference-free Tactile Monitoring on Skins,” *Science Advances* 7 (2021): abi4563, <https://doi.org/10.1126/sciadv.abi4563>.
132. S. Duan, F. Zhao, P. Chen, J. Liu, L. Liu, and J. Wu, “Stretchable Adhesive E-skin with Decoupled Pressure-strain Sensing,” *Device* (2026): 101069, <https://doi.org/10.1016/j.device.2026.101069>.
133. L. Wen, M. Nie, P. Chen, et al., “Wearable Multimode Sensor with a Seamless Integrated Structure for Recognition of Different Joint Motion States with the Assistance of a Deep Learning Algorithm,” *Microsystems & Nanoengineering* 8 (2022): 24, <https://doi.org/10.1038/s41378-022-00358-2>.
134. H. N. Wang, X. F. Liu, D. Chen, et al., “Strain Redistribution Effect Based Composite Structured Sensor for Decouplable Tactile-Strain Double-Mode Perception,” *Advanced Sensor Research* 4 (2025): 2400147, <https://doi.org/10.1002/adsr.202400147>.
135. X. H. Zheng, S. L. Zhang, M. J. Zhou, et al., “MXene Functionalized, Highly Breathable and Sensitive Pressure Sensors with Multi-Layered Porous Structure,” *Advanced Functional Materials* 33 (2023): 2214880, <https://doi.org/10.1002/adfm.202214880>.
136. J. Xu, H. Y. Li, Y. M. Yin, et al., “High Sensitivity and Broad Linearity Range Pressure Sensor Based on Hierarchical in-situ Filling Porous Structure,” *npj Flexible Electronics* 6 (2022): 62, <https://doi.org/10.1038/s41528-022-00191-7>.
137. S. Wang, C. Wang, Y. Zhao, et al., “Flexible Pressure Sensors with Ultrahigh Stress Tolerance Enabled by Periodic Microslits,” *Microsystems & Nanoengineering* 10 (2024): 24, <https://doi.org/10.1038/s41378-023-00639-4>.
138. Y. Xiao, Y. Duan, N. Li, et al., “Multilayer Double-Sided Microstructured Flexible Iontronic Pressure Sensor with a Record-wide Linear Working Range,” *ACS Sensors* 6 (2021): 1785–1795, <https://doi.org/10.1021/acssensors.0c02547>.
139. L. Wen, W. T. Fan, J. H. Kang, and H. Z. Huang, “Porous Pressure Sensors from Mechanisms to Application: a Review,” *Sensors and Actuators A: Physical* 387 (2025): 116461, <https://doi.org/10.1016/j.sna.2025.116461>.
140. Y. Ding, T. Xu, O. Onyilagha, H. Fong, and Z. Zhu, “Recent Advances in Flexible and Wearable Pressure Sensors Based on Piezoresistive 3D Monolithic Conductive Sponges,” *ACS Applied Materials & Interfaces* 11 (2019): 6685–6704, <https://doi.org/10.1021/acsami.8b20929>.
141. H. Zhang, C. Yang, H. Xia, W. An, M. Qi, and D. Zhang, “Layer-by-Layer Self-Assembled Honeycomb Structure Flexible Pressure Sensor Array for Gait Analysis and Motion Posture Recognition with the Assistance of the ResNet-50 Neural Network,” *ACS Sensors* 10 (2025): 2358–2366, <https://doi.org/10.1021/acssensors.5c00187>.
142. T. C. Huang, R. L. Wei, Q. L. Hua, Z. Q. Yuan, and G. Z. Shen, “A Smart Sponge with Pressure–Temperature Dual-Mode Sensing for Packaging and Transportation,” *Chemical Engineering Journal* 499 (2024): 156292, <https://doi.org/10.1016/j.cej.2024.156292>.
143. H. B. Yao, J. Ge, C. F. Wang, et al., “A Flexible and Highly Pressure-Sensitive Graphene–Polyurethane Sponge Based on Fractured Microstructure Design,” *Advanced Materials* 25 (2013): 6692–6698, <https://doi.org/10.1002/adma.201303041>.
144. J. Ai, S. R. Cheng, Y. J. Miao, P. Li, and H. X. Zhang, “Graphene/Electrospun Carbon Nanofiber Sponge Composites Induced by Magnetic Particles for Multi-functional Pressure Sensor,” *Carbon* 205 (2023): 454–462, <https://doi.org/10.1016/j.carbon.2023.01.033>.
145. C. Y. Li, H. Gu, Z. Y. Ji, et al., “Hierarchically Structured MXene Nanosheets on Carbon Sponges with a Synergistic Effect of Electrostatic Adsorption and Capillary Action for Highly Sensitive Pressure Sensors,” *ACS Applied Nano Materials* 6 (2023): 13482–13491, <https://doi.org/10.1021/acsnm.3c02126>.
146. Y. Ding, J. Yang, C. R. Tolle, and Z. Zhu, “Flexible and Compressible PEDOT:PSS@Melamine Conductive Sponge Prepared via One-Step Dip Coating as Piezoresistive Pressure Sensor for Human Motion Detection,” *ACS Applied Materials & Interfaces* 10 (2018): 16077–16086, <https://doi.org/10.1021/acsami.8b00457>.
147. W. Li, X. Jin, X. Han, et al., “Synergy of Porous Structure and Microstructure in Piezoresistive Material for High-Performance and Flexible Pressure Sensors,” *ACS Applied Materials & Interfaces* 13 (2021): 19211–19220, <https://doi.org/10.1021/acsami.0c22938>.
148. M. Y. Zhang, W. K. Yang, Z. Q. Wang, et al., “Highly Compressible and Thermal Insulative Conductive MXene/PEDOT:PSS@Melamine Foam for Promising Wearable Piezoresistive Sensor,” *Applied Physics Letters* 122 (2023): 043507, <https://doi.org/10.1063/5.0137571>.
149. W. Guo, Z. Q. Ma, Z. Chen, et al., “Thin and Soft Ti₃C₂T_x MXene Sponge Structure for Highly Sensitive Pressure Sensor Assisted by Deep Learning,” *Chemical Engineering Journal* 485 (2024): 149659, <https://doi.org/10.1016/j.cej.2024.149659>.
150. J. Byun, Y. Lee, J. Yoon, et al., “Electronic Skins for Soft, Compact, Reversible Assembly of Wirelessly Activated Fully Soft Robots,” *Science Robotics* 3 (2018): aas9020, <https://doi.org/10.1126/scirobotics.aas9020>.
151. S. Sundaram, P. Kellnhofer, Y. Li, J. Y. Zhu, A. Torralba, and W. Matusik, “Learning the Signatures of the Human Grasp Using a Scalable Tactile Glove,” *Nature* 569 (2019): 698–702, <https://doi.org/10.1038/s41586-019-1234-z>.
152. Y. C. Huang, Y. Liu, C. Ma, et al., “Sensitive Pressure Sensors Based on Conductive Microstructured Air-gap Gates and Two-dimensional Semiconductor Transistors,” *Nature Electronics* 3 (2020): 59–69, <https://doi.org/10.1038/s41928-019-0356-5>.
153. Q. Wu, Y. Qiao, R. Guo, et al., “Triode-Mimicking Graphene Pressure Sensor with Positive Resistance Variation for Physiology and Motion Monitoring,” *ACS Nano* 14 (2020): 10104–10114, <https://doi.org/10.1021/acsnano.0c03294>.
154. S. Min, J. An, J. H. Lee, et al., “Wearable Blood Pressure Sensors for Cardiovascular Monitoring and Machine Learning Algorithms for Blood Pressure Estimation,” *Nature Reviews Cardiology* 22 (2025): 629–648, <https://doi.org/10.1038/s41569-025-01127-0>.
155. S. Li, H. Wang, W. Ma, et al., “Monitoring Blood Pressure and Cardiac Function without Positioning via a Deep Learning-Assisted Strain Sensor Array,” *Science Advances* 9 (2023): adh0615, <https://doi.org/10.1126/sciadv.adh0615>.
156. L. Yang, H. Wang, W. Yuan, et al., “Wearable Pressure Sensors Based on MXene/Tissue Papers for Wireless Human Health Monitoring,” *ACS*

- Applied Materials & Interfaces* 13 (2021): 60531–60543, <https://doi.org/10.1021/acssami.1c22001>.
157. Z. Sang, K. Ke, and I. Manas-Zloczower, “Design Strategy for Porous Composites Aimed at Pressure Sensor Application,” *Small* 15 (2019): 1903487, <https://doi.org/10.1002/smll.201903487>.
158. Y. Cotur, S. Olenik, T. Asfour, et al., “Bioinspired Stretchable Transducer for Wearable Continuous Monitoring of Respiratory Patterns in Humans and Animals,” *Advanced Materials* 34 (2022): 2203310, <https://doi.org/10.1002/adma.202203310>.
159. D. Kim, J. Lee, M. K. Park, and S. H. Ko, “Recent Developments in Wearable Breath Sensors for Healthcare Monitoring,” *Communications Materials* 5 (2024): 41, <https://doi.org/10.1038/s43246-024-00480-w>.
160. J. Liu, F. Wang, Q. Zhao, and Y. Liu, “Multifunctional Conductive Hydrogels Based on the Alkali Lignin-Fe³⁺-Mediated Fenton Reaction for Bioelectronics,” *International Journal of Biological Macromolecules* 235 (2023): 123817, <https://doi.org/10.1016/j.ijbiomac.2023.123817>.
161. H. Xu, L. Gao, H. Zhao, et al., “Stretchable and Anti-impact Iontronic Pressure Sensor with an Ultrabroad Linear Range for Biophysical Monitoring and Deep Learning-aided Knee Rehabilitation,” *Microsystems & Nanoengineering* 7 (2021): 92, <https://doi.org/10.1038/s41378-021-00318-2>.
162. C. Moreau, T. Rouaud, D. Grabli, et al., “Overview on Wearable Sensors for the Management of Parkinson’s Disease,” *npj Parkinson’s Disease* 9 (2023): 153, <https://doi.org/10.1038/s41531-023-00585-y>.
163. T. Rafeedi, A. Abdal, B. Polat, K. A. Hutcheson, E. H. Shinn, and D. J. Lipomi, “Wearable, Epidermal Devices for Assessment of Swallowing Function,” *npj Flexible Electronics* 7 (2023): 52, <https://doi.org/10.1038/s41528-023-00286-9>.
164. O. Gul, J. Kim, K. Kim, H. J. Kim, and I. Park, “Liquid-Metal-Based Soft Pressure Sensor and Multidirectional Detection by Machine Learning,” *Advanced Materials Technologies* 9 (2024): 2302134, <https://doi.org/10.1002/admt.202302134>.
165. J. V. Vaghasiya, C. C. Mayorga-Martinez, J. Vyskocil, and M. Pumera, “Black Phosphorous-Based Human-Machine Communication Interface,” *Nature Communications* 14 (2023): 2, <https://doi.org/10.1038/s41467-022-34482-4>.
166. M. J. Zhong, L. J. Zhang, X. Liu, et al., “Wide Linear Range and Highly Sensitive Flexible Pressure Sensor Based on Multistage Sensing Process for Health Monitoring and Human-Machine Interfaces,” *Chemical Engineering Journal* 412 (2021): 128649, <https://doi.org/10.1016/j.cej.2021.128649>.
167. J. Kim, M. Lee, H. J. Shim, et al., “Stretchable Silicon Nanoribbon Electronics for Skin Prosthesis,” *Nature Communications* 5 (2014): 5747, <https://doi.org/10.1038/ncomms6747>.
168. Y. D. Yang, Y. Liu, and R. Yin, “Fiber/Yarn and Textile-Based Piezoresistive Pressure Sensors,” *Advanced Fiber Materials* 7 (2025): 34–71, <https://doi.org/10.1007/s42765-024-00479-5>.
169. Q. Liu, Y. Zhang, X. Sun, et al., “All Textile-Based Robust Pressure Sensors for Smart Garments,” *Chemical Engineering Journal* 454 (2023): 140302, <https://doi.org/10.1016/j.cej.2022.140302>.
170. Q. Shi, Z. Zhang, T. He, et al., “Deep Learning Enabled Smart Mats as a Scalable Floor Monitoring System,” *Nature Communications* 11 (2020): 4609, <https://doi.org/10.1038/s41467-020-18471-z>.
171. D. D. Guo, Y. L. Li, Q. H. Zhou, et al., “Degradable, Biocompatible, and Flexible Capacitive Pressure Sensor for Intelligent Gait Recognition and Rehabilitation Training,” *Nano Energy* 127 (2024): 109750, <https://doi.org/10.1016/j.nanoen.2024.109750>.
172. L. Zhu, Y. Wang, D. Mei, and C. Jiang, “Development of Fully Flexible Tactile Pressure Sensor with Bilayer Interlaced Bumps for Robotic Grasping Applications,” *Micromachines* 11 (2020): 770, <https://doi.org/10.3390/mi11080770>.
173. J. Shintake, V. Cacucciolo, D. Floreano, and H. Shea, “Soft Robotic Grippers,” *Advanced Materials* 30 (2018): 1707035, <https://doi.org/10.1002/adma.201707035>.
174. Z. E. Zhang, Z. T. Zhang, D. Q. Mei, and Y. C. Wang, “Multifunctional Flexible Sensor with both Contact Pressure Sensing and Internal Ultrasonic Detection for Robotic Grasping,” *Sensors and Actuators A: Physical* 383 (2025): 116202, <https://doi.org/10.1016/j.sna.2025.116202>.
175. B. Q. Jia, Z. K. Li, T. F. Zheng, et al., “Highly-Sensitive, Broad-Range, and Highly-Dynamic MXene Pressure Sensors with Multi-level Nanostructures for Healthcare and Soft Robots Applications,” *Chemical Engineering Journal* 485 (2024): 149750, <https://doi.org/10.1016/j.cej.2024.149750>.
176. J. T. Qu, G. M. Cui, Z. K. Li, et al., “Advanced Flexible Sensing Technologies for Soft Robots,” *Advanced Functional Materials* 34 (2024): 2401311, <https://doi.org/10.1002/adfm.202401311>.
177. C. Hegde, J. Su, J. M. R. Tan, K. He, X. Chen, and S. Magdassi, “Sensing in Soft Robotics,” *ACS Nano* 17 (2023): 15277–15307, <https://doi.org/10.1021/acsnano.3c04089>.
178. R. L. Truby, M. Wehner, A. K. Grosskopf, et al., “Soft Somatosensitive Actuators via Embedded 3D Printing,” *Advanced Materials* 30 (2018): 1706383, <https://doi.org/10.1002/adma.201706383>.
179. Y. Y. Hou, Y. H. Xu, Z. M. Cai, et al., “Decoupled Approaches for Multimodal Flexible Sensor Systems,” *Nano Research* 18 (2025): 94907673, <https://doi.org/10.26599/NR.2025.94907673>.
180. T. Wu, Y. T. Li, L. Zhao, et al., “Recent Progress on Flexible Multimodal Sensors: Decoupling Strategies, Fabrication and Applications,” *Advanced Materials* 38 (2026): 21375, <https://doi.org/10.1002/adma.202521375>.
181. B. Jafarizadeh, A. H. Chowdhury, M. S. I. Sozal, Z. Cheng, N. Pala, and C. L. Wang, “Hardware and Protocol for Testing of Piezoresistive Pressure Sensors for Pulse Wave Monitoring,” *IEEE Sensors Letters* 7 (2023): 1–4, <https://doi.org/10.1109/LESENS.2023.3300826>.
182. S. J. Hong, Y. R. Lee, A. Bag, et al., “Bio-inspired Artificial Mechanoreceptors with Built-in Synaptic Functions for Intelligent Tactile Skin,” *Nature Materials* 24 (2025): 1100–1108, <https://doi.org/10.1038/s41563-025-02204-y>.
183. L. Chen, S. Karilanova, S. Chaki, et al., “Spike Timing-Based Coding in Neuromimetic Tactile System Enables Dynamic Object Classification,” *Science* 384 (2024): 660–665, <https://doi.org/10.1126/science.adf3708>.
184. S. Chen, Z. Zhou, K. Hou, et al., “Artificial Organic Afferent Nerves Enable Closed-Loop Tactile Feedback for Intelligent Robot,” *Nature Communications* 15 (2024): 7056, <https://doi.org/10.1038/s41467-024-51403-9>.
185. D. Hardman, T. G. Thuruthel, and F. Iida, “Multimodal Information Structuring with Single-Layer Soft Skins and High-Density Electrical Impedance Tomography,” *Science Robotics* 10 (2025): adq2303, <https://doi.org/10.1126/scirobotics.adq2303>.
186. K. K. Kim, T. J. Zaluska, S. Skov, et al., “A Simplified Wearable Device Powered by a Generative EMG Network for Hand-Gesture Recognition and Gait Prediction,” *Nature Sensors* 1 (2025): 27–38, <https://doi.org/10.1038/s44460-025-00002-2>.
187. G. Yun, Z. Chen, Z. Chen, et al., “Multiscale-structured Miniaturized 3D Force Sensors,” *Nature Materials* 240 (2026): 1–11, <https://doi.org/10.1038/s41563-026-02508-7>.
188. J. R. Huang, Y. C. Guo, Y. C. Jiang, F. Y. Wang, L. J. Pan, and Y. Shi, “Recent Advances and Future Prospects in Tactile Sensors for Normal and Shear Force Detection, Decoupling, and Applications,” *Journal of Semiconductors* 45 (2024): 121601.
189. F. Yu, Q. Liu, X. Gan, et al., “Ultrasensitive Pressure Detection of Few-Layer MoS₂,” *Advanced Materials* 29 (2017): 1603266, <https://doi.org/10.1002/adma.201603266>.

Biographies



Feng Luo is a postdoctoral researcher at the University of Strasbourg. He received his bachelor's and master's degrees from Chongqing University in 2021 and his Ph.D. in physical chemistry from the University of Strasbourg, France in 2025. His research interests include 2D materials and structural engineering, flexible sensors for human-machine interaction and health monitoring, and AI-assisted data acquisition and processing system.



Artur Ciesielski is a CNRS Research Director at the Institut de Science et d'Ingénierie Supramoléculaires (ISIS) at the Université de Strasbourg in France and a Visiting Professor at the Center for Advanced Technologies at Adam Mickiewicz University in Poznań, Poland. His research focuses on the design, synthesis, and application of functional two-dimensional (2D) materials, including graphene, covalent-organic frameworks (COFs), and transition metal dichalcogenides, for energy storage, sensing, and environmental applications.



Paolo Samori is Distinguished Professor at the University of Strasbourg and Director of the Institut de Science et d'Ingénierie Supramoléculaires. He is Member of the Académie des technologies, Member of ACATECH, Fellow of the Royal Society of Chemistry (FRSC), Fellow of the European Academy of Sciences (EURASC), Member of the Academia Europaea, Fellow of the Materials Research Society (MRS), Foreign Member of the Royal Flemish Academy of Belgium for Science and the Arts (KVAB), and Senior Member of the Institut Universitaire de France (IUF). His research interests comprise nanochemistry, supramolecular sciences, materials chemistry with specific focus on graphene and 2D semiconductors, functional organic/polymeric and hybrid nanomaterials for application in optoelectronics, energy and sensing.